IJBST

ISSN: 0974 – 3987
IJBST (2009), 2(7): 96-125

# Automatic Detection of diagnostic features using real-time ECG signals: Application to patients prone to Cardiac Arrhythmias

G. K. Singh[1], A. Sharma[2], S. Velusami[3]

1Professor, Department of Electrical Engineering, Indian Institute of Technology, Roorkee, 247667, Uttarakhand, INDIA
2 Assistant Professor, Department of Electrical Engineering, Indian Institute of Technology, Roorkee, 247667, Uttarakhand, INDIA
3 Professor, Department of Electrical Engineering, Annamalai University, Annamalainagar, 608002, Tamilnadu, INDIA.
gksngfee@gmail.com, Fax: +91-1332-272560, Phone +91-1332-285070

**ABSTRACT**

A composite method for the automatic detection of diagnostic features related to the depolarization sequence (P-QRS complex) of the heart, for arrhythmia classification, using single lead ECG is presented. The non-syntactic approach based upon slope and amplitude thresholds along with a set of empirical criteria is employed for segmenting QRS complexes from a variety of noisy ECG recordings acquired from the MIT/BIH arrhythmia database. The background noise is removed from the non-QRS portions using an appropriate filtering method that causes no change in the amplitudes or boundaries of P and T waves. In R-R intervals, the isoelectric line is determined by developing a technique based upon the method of least squares approximation. Amplitude threshold bands are set up above and below the isoelectric line to detect P and /or T wave peaks. Using a group of decision logic rules, framed on the basis of an exhaustive study of normal and arrhythmic ECG signals and detailed consultations with two independent cardiologists, the P waves are discriminated from the T waves. In total, 37 useful diagnostic features have been deduced pertaining to the QRS and P waves in the time domain. The QRS detection algorithm of the composite method was validated using 32,800 beats of several records of the MIT/BIH database for which a detection accuracy of 99.96% was achieved within the tolerance limits recommended by the CSE Working Party. The composite method for detection of both P and QRS wave features has been validated using all the 25 records for lead II of the CSE Dataset-3, before being applied to approximately 8000 beats of the MIT/BIH database. As regards noisy signals, only those were analysed that had a baseline wander not exceeding 0.25 Hz**.**

**Keywords:** Arrhythmia, ECG signal, P-QRS complex, MIT/BIH data base, atrio-ventricular conduction ratio, diagnostic feature

## INTRODUCTION

Cardiac arrhythmias occur when disturbances are caused in the normal electrical events related to the basic processes of automaticity, conduction and triggering mechanisms of the heart [1, 2]. If not well diagnosed in time, they represent a serious threat to the patient. Therefore, there is a need for quick identification of these abnormal electrical activities of the heart. Both life threatening (e.g. ventricular fibrillation and atrial fibrillation) and not-so-life threatening arrhythmias (e.g. premature ventricular contraction and atrial premature contraction) can be detected by using the electrocardiogram (ECG) that is a low-cost, non-invasive and standard diagnostic measure employed by cardiologists all over the world.

A standard ECG record is the best test for diagnosing all arrhythmias, whether of ventricular or supraventricular origin. An ECG tracing is a series of waves that represent the electrical events of the various chambers and conduction pathways within the heart. The electrical activity during the cardiac cycle is characterized by five separate waves of deflections designated as P, Q, R, S and T. The configuration of one complete ECG cycle or beat demonstrating the wave intervals and segments normally observed in the ECG is shown in Fig. 1.

A normal ECG rhythm is an ordered sequence of depolarisation of the myocardial cells [3], i.e. the sequence of P wave (atrial myocardial depolarisation) and QRS wave (ventricular myocardial depolarisation) generation, at a regular rate of 60-100 beats per minute (bpm). When this sequence is disturbed, it is manifested as an irregularity in the heart rate or ECG morphology. As a result, abnormal rhythms or arrhythmias occur.

Rhythms analysis to diagnose arrhythmias involves the accurate detection of P waves and QRS complexes with respect to time, with respect to each other and with respect to space [3, 4]. Arrhythmia monitoring is performed generally using ECG lead II, since both the P waves and QRS complexes are observed clearly in this lead [1-6].

Computer based rhythm analysis is the state-of-the-art technology assisting cardiologists and physicians now-a-days. A large number of algorithms have been developed by researchers to combat the problems cardiologists face while performing the tedious task of

visual interpretation of Holter ECG records. The work carried out in this paper is another attempt at automated extraction of diagnostic features from ECG signal that would help the cardiologist to perform reliable arrhythmia detection.

A composite methodology has been developed in the time domain that extracts 37 useful diagnostic features from ECG signal which is an improvement over previously reported algorithms [7-23] used for analysing the ECG signals of the MIT/BIH standard arrhythmia database.

## CHARACTERISTICS OF MIT/BIH ARRHYTHMIA DATABASE

The MIT/BIH database consists of roughly 109,000 beats that have been manually annotated by at least two cardiologists working independently. The reference annotation files, include beat, rhythm, and signal quality annotations. Each signal file contains two signals sampled at 360 Hz.

Modified lead II (MLII) has been provided as one of the two channel ECG recordings [24]. Most of the arrhythmia detection algorithms reported in literature have opted MLII for performing QRS detection and rhythm analysis [9, 15, 18, 25]. However, ECG record segments, with poor signal quality and corrupted by high noise have generally been excluded from rigorous analysis due to the deteriorating performance of the QRS detection software while processing these records to accomplish arrhythmia detection [6, 10, 13, 18, 20, 24, 26].

It is to be noted that real time ECG signals of the MIT/BIH database are largely contaminated by different frequencies of noise, viz., baseline wander in the range of 0.05 to 0.8 Hz, most of the signals having a baseline drift well below 0.5 Hz [6,12,26-29]; motion artifacts below 7 Hz [12]; powerline interference at 60 Hz, and multiples of 30 Hz [24]; and other high frequency noise, like muscle noise in the range 50 Hz to 2 kHz [18,30,31].

The most useful diagnostic components of the ECG signal, for arrhythmia analysis, the P wave and the QRS complex, also lie within these frequency ranges. The relative power spectra of QRS complex lies approximately within 5 to 25 Hz, the maximum QRS energy being around 17 Hz, while P and T waves lie in the frequency range below 10 Hz [6, 12, 25, 26, 32]. Therefore, while removal of the multiple frequency noise, it is very important to decide how much to filter, i.e. how to preserve the “true” signal content to be used for diagnostics, while eliminating noise that interferes during the process of feature extraction [18,28,33].

Another important aspect, related to the annotated ECG records of the MIT/BIH database is that the database does not provide any measurement data that can be utilized to verify the magnitudes and boundaries of different features extracted (e.g. QRS-onset, QRS-offset, P-onset, P-offset).

Manual measurements or seeking help from a cardiologist are the only ways to verify the extracted QRS and P wave features. In this scenario, an attempt has been made to develop a method for automated feature extraction in the time domain using real-time MLII ECGs of the MIT/BIH database.

However, prior to rigorous testing and application of the QRS and P wave detection algorithms using the records of the MIT/BIH database; these algorithms were validated using the 25 records of the CSE Dataset-3 for which the measurement data are provided [34].

## PRESENT METHODOLGY FOR ECG PROCESSING

### Composite Method of Feature Extraction

The technique developed performs cycle-by-cycle or R-R interval by R-R interval feature extraction from the given real-time ECG signal to enable interpretation of different arrhythmias. Cycle-by-cycle feature extraction helps the cardiologist while diagnosing one arrhythmia (e.g. sinus bradycardia, atrial fibrillation) at a time, or a combination of two or more arrhythmias (e.g. sinus bradycardia with right bundle branch block) coexisting in the signal.

Also, this approach aids the cardiologist in detecting multiple arrhythmias in the same sequence as they appear in the ECG signal under examination.

The composite methodology developed for automated extraction of both QRS and P wave features for arrhythmia classification, comprises of following major elements:

- Extraction of QRS complex from noisy non-QRS segments in the ECG signal; extraction of QRS complex features such as peak (Q,R,S) amplitudes, QRS onset and offset etc.; derivation of associated features such as R-R interval, heart rate, QRS configuration etc

- Digital filtering of noisy non-QRS segments

- Detection of iso-electric (IE) line in R-R interval; IE line is used as reference base line to detect peaks present in non-QRS segments in R-R interval

- Extraction of P wave and associated features from non-QRS segments of R-R intervals using decision logic rules (employed to discriminate between P and T waves); detection of features such as P wave position and polarity, P wave onset and offset, and derivation of associated features such as P-R interval and P-P interval, etc.

The complete procedure implemented, in the present study, is outlined in Fig. 2. The QRS detection algorithm, developed in the present study, first identifies the R peak point in the QRS complex. Using the detected R peak point as a reference, the algorithm is further extended to detect other component peaks of the QRS complex, QRS onset and offset and other associated diagnostic features.

The detection of P waves in the ECG signal involves a pre-processing stage that eliminates noise and smoothens the non-QRS segment present in R-R interval. Thereafter, the IE line is computed for each R-R interval to account for abrupt changes in baseline of the ECG signal.

A point of inflexion in smoothened non-QRS segment is taken as a P or T peak point if it falls within the amplitude threshold band limits defined above and below the computed IE line. The P peak is discriminated from T peak using a set of decision logic rules developed in the present study. The technique eventually computes the diagnostic features associated with the P wave. Important details of the composite method are as follows:

**ECG Segmentation – Extraction of QRS Complex**

QRS complexes are extracted from the noisy ECG signals using a method developed, based on the very widely employed non-syntactic approach: the amplitude and slope threshold technique [13,14, 18, 30, 32, 35-38] that is immune to low-amplitude noise corrupting the non-QRS portions of ECG signals, and provides successful QRS detection in the presence of moderate baseline wander.

The frequency spectrum of the QRS complexes overlaps that of the noise contaminating non-QRS segments. Hence, QRS complexes are segmented out from the noisy ECGs and analysed separately from the remaining non-QRS noisy portions of the ECG signal that need to be filtered before further processing to detect P waves.

The background noise is rejected by QRS detection procedure that is based on computing the slope that lies within a certain threshold. The slope is computed using first difference for an optimized number of seven consecutive samples along the rising R wave, and the change in its sign is observed.

At the point of inflexion, sign of the slope changes from positive to negative (or vice versa). This point of transition is taken to be a possible QRS complex peak, however, its final detection is subject to certain additional criteria consisting of decision rules providing optimum thresholds that characterise various QRS wave features.

These criteria are formulated in the present methodology on the basis of standards of ECG interpretation [1-3, 26, 35, 37], recommendations of the CSE Working Party [39], statistical variation of the ECG data processed in the present study, and extensive trial-and-error tests conducted over a large quantity of ECG data.

These additional criteria are as follows:

(a) The general configuration of the QRS complex (with upright R wave), in the MLII ECG signals, contains Q-R-S-R' peaks in a sequence. Therefore, a detected QRS complex may be a peak complex [39, 40], having the following morphologies: QRS, QR, RS, R, RSR', QRSR', QS (Table 1). Annotated beats in the MIT/BIH database with single negative waves have been termed in the present study as QS waves,

(b) QRS onset has been used as the reference point for determining the base level to perform all amplitude measurements pertaining to QRS complex [39],

(c) R' peak cannot exist without S peak in a QRS complex [36, 40],

(d) ECG signals with acceptable noise levels can be subjected to noise thresholding to detect Q, S and R' peaks in presence of noisy peaks of low amplitude [37, 40, 41]. After extensive tests conducted over a large number of ECG data, an optimized amplitude threshold of 0.06 mV was determined for differentiating Q, S and R' peaks from noisy ECG peaks (Daskolov et al. [37] have used an amplitude threshold of 0.05 mV to differentiate the component peaks of QRS complex from noisy peaks. The difference between the amplitude thresholds arrived at in the present study and that of Daskalov et al. may be attributed to the fact that their study was carried

out using a 12 lead recorded data instead of the 2 lead MIT/BIH database used in the present study), ie.:

- Any negative peak before the R peak, with an amplitude of 0.06 mV or greater with respect to (w.r.t.) the QRS onset, is the Q peak
- Any negative peak after the R peak, with an amplitude of 0.06 mV or greater w.r.t. QRS offset, is the S peak
- Any positive peak after the S peak, with an amplitude 0f 0.06 mV or greater w.r.t. the QRS offset, is the R' peak

(e) The noise corrupted nature of ECG signal is utilized for detecting onset and offset of QRS complex. Onset of Q wave (if present) is the onset of QRS complex at a point where the slope threshold of QRS wave changes or the slope becomes nearly zero [35, 37]; onset of R wave is the onset of QRS complex if Q wave is absent. Similarly, offset of QRS complex is the offset of R' wave (if present) or is offset of S wave when R' wave is absent or is the offset of R wave when S wave is absent,

(f) A slur or a notch may occur at any sample point either along the rising or falling limb of the component waves (Q, R, S and R′), interfering with computation of onsets, offsets and peak extremums of these waves. Fig. 3 shows eight types of notched and slurred wave configurations, where A, C, E and G are slurs, and, B, D, F and H are notches that may be encountered in the QRS complexes. To deal with this practical situation a suitable method is employed to test for the QRS boundaries, slurs and notches. Mainly, a check is made for the calculation of the respective peak points, offsets and onsets. For instance, if a deflection (C or D type) occurs in the rising limb of the S wave, then for next few data samples beyond this deflection, it is checked whether the upward slope continues within a threshold or not. If it continues, then the deflection encountered in the wave is specified a slur /notch, and the search is further carried out to detect the offset of S wave or peak extremum of R' wave. If the upward slope does not continue within a threshold for a few data samples beyond this deflection, then the first sample point of the occurrence of this deflection is marked as the offset of S wave, and hence the offset of QRS complex. In a similar manner, other types of slurs and notches may be distinguished from the onsets, offsets and peak extremums of Q, R, S and R' waves. This technique was tested on slurs and notches of small magnitudes,

(g) In more than 90% of the QRS complexes of the MIT/BIH database records (having a baseline wander in the range of 0.05 Hz to 0.25 Hz), analysed in the present study to calculate QRS duration, it was found that the amplitudes of QRS onset and offset differed within a range of 0.1 mV. Therefore, this range was utilized to detect different features of the QRS complex such as QRS offset, S peak and R' peak in presence of notches and slurs. Results of the computations of the QRS duration measured from its onset to offset, after implementing the above condition, were found to be within the prescribed tolerance limits [39],

(h) In case a T wave occurs with a magnitude comparable to that of the preceding QRS complex, the criteria used by Pan and Tompkins [13] is employed to discriminate between the T wave and QRS complex.

The step-by-step procedure developed for detection of QRS complex and associated features is illustrated in Fig. 4.

**Digital Filtering of non-QRS Segments**

The non-QRS portions of the MLII ECG signals are corrupted by noise. This noise was removed to identify P and T peaks, and subsequently extract only P waves using the technique of amplitude and slope threshold criteria. For computation of slope, the simplest technique of first difference has been used that performs very well for noise free signals [32].

In the present study, a $6^{th}$-order low pass Butterworth digital filter having a cut-off frequency of 10 Hz is used to remove the noise in the non-QRS segments of the acquired real-time ECGs. Its amplitude response with cut off frequency of 10 Hz is shown in Fig. 5.

This $6^{th}$-order IIR (infinite impulse response) digital filter is a cascade combination of three $2^{nd}$-order filter sections, each $2^{nd}$-order section generating a separate set of five digital filter coefficients that are used to produce a noise free signal. The filter design is accomplished by the algorithm developed by Stearns and David [42]. The primary advantages of this filter are its sharp frequency cut-off and stability [6, 42].

To select an optimum cut-off frequency for filtering noise in the non-QRS segments by the low pass Butterworth filter, Fast Fourier Transform (FFT) was computed for a large set of these segments acquired from different records of the MIT/BIH database.

From these FFT responses, it was found that the frequency content of P and T waves lies within 10 Hz. Hence, 10 Hz was selected as the optimum low-pass filter frequency cut-off. It was also observed that this low pass filter scheme provides noise free and smoothened signal with no substantial amplitude attenuation of P and T peaks and no change in the R-R and P-P intervals.

**Detection of IE Line in R-R Intervals**

The imaginary IE line in an R-R interval is determined between two consecutive QRS complexes of the filtered ECG. It is used as a reference base line to detect P and T peaks. However, only P wave parameters have been extracted from the non-QRS interwave segments of R-R intervals.

Based on the recommendations to determine a reference baseline [39], a technique has been developed to determine an IE line in an R-R interval. However, it is to be noted that in the arrhythmic ECG signals of the MIT/BIH database, the P wave may fuse with QRS onset or may not be present at all (e.g. Premature Ventricular Complex- PVCs, ventricular tachycardia etc.) in some portions of the signal under analysis.

In such cases, the P-R segment criteria for determining the IE line cannot be implemented. Therefore, the technique determines an IE line that passes through samples within a certain amplitude threshold using the onset of QRS complex as a reference point. These samples lie in the window having a maximum length of 66% of R-R interval starting from the onset of QRS complex.

Macfarlene et al. [43] used linear interpolation to determine the baseline in ECG signals. In this study too, a straight line is fitted using the technique of least squares approximation [42] by scanning the samples located in the window. The onset and offset of this imaginary IE line are then, respectively, compared with the detected offset of previous QRS complex and onset of current QRS complex.

If the comparison satisfies a stipulated threshold (that was arrived at after extensive trial and error tests on a large number of ECG data with moderate baseline wander lying within 0.05 to 0.25 Hz), then the fitted imaginary IE line is taken to be finally detected, otherwise the window size for the R-R interval is modified (in terms of both the length and height of the window). The window size is modified (i.e., the window size contracts or expands sequentially) a maximum of four times in order to detect a horizontal /slant imaginary IE line. The step-by-step procedure for detection of IE line between two consecutive QRS complexes is illustrated in Fig. 6.

**P Wave Extraction from ECG Signal**

In most of the arrhythmia monitoring systems the next step after valid QRS complex recognition is P wave detection followed by extraction of P wave features. Extraction of low amplitude P waves in a noise corrupted ECG has posed problems in several arrhythmia detectors. Therefore, most arrhythmia monitors used in hospitals and clinics depend on features related to QRS complex only, like R-R interval, heart rate, QRS duration etc. [2, 3, 6, 31, 35, 44].

However, in the present study, P wave detection (based on the amplitude and slope threshold criteria) has been successfully performed, whatever is its magnitude, polarity or location in an R-R interval, since, non-QRS segments are filtered and smoothened prior to P wave extraction. The methodology for detection of P waves and associated features is illustrated in Fig. 7.

Amplitude threshold band limits above and below the computed IE lines have been determined to identify undulations and peaks of P and T waves. Undulations are very small P waves having magnitudes much smaller than those of the normal P waves. These are also known as the fibrillatory waves [1, 2, 45, 46].

In this work, a technique has been developed to detect P and T peaks between two consecutive QRS complexes based on an algorithm, which follows a set of decision logic rules. This technique discriminates well between P and T waves so that the next set of useful diagnostic features pertaining to the P wave and its relationship to the QRS complex is easily determined.

The P wave parameters like P peak location and amplitude and P wave onset and offset location and amplitude are determined on the basis of slope computations performed on the filtered non-QRS segments. As per the CSE recommendations, P onset has been used as a reference point to determine the base level for P wave amplitude measurements.

**Decision Logic Rules to Discriminate Between P and T Waves**

It is well known that in arrhythmic signals, P and T waves have inconsistent locations w.r.t. the QRS complex in successive R-R intervals. For example, abnormal rhythms like bigeminy, trigeminy, ventricular tachycardia or multiple arrhythmia signals

display irregularities in locations of P and T waves. In such cases, it is very difficult to detect whether a wave is a P wave or a T wave in an R-R interval. Absence of universally accepted criteria for detecting the difference between P and T wave, and the need for designing an automatic real time procedure that would distinguish between the two waves has motivated towards the development of decision logic rules for the purpose.

Different decision logic rules have been developed for discriminating between P and T peaks in an R-R interval after an exhaustive study of arrhythmia signals in the MIT/BIH arrhythmia database and arrhythmic ECG signals available in literature [1-5, 24, 46]. Consultations with two experienced cardiologists were also made in this regard.

With the help of these rules /conditions, presence, polarity, position and number of P/T waves /peaks, w.r.t. midpoint in an R-R interval can be detected. All these conditions are represented by a parameter termed as 'FLAG'.

The position of midpoint in an R1-R2 interval is computed as equal to $(QRS1_{of} + QRS2_{on})/2$, where $QRS1_{of}$ is offset of the QRS1 complex and $QRS2_{on}$ is onset of the QRS2 complex. A positive peak (P/T) is a peak above (upright wave) the detected IE line, and a negative peak (P/T) is one below (downright wave) this line.

These decision logic rules are summarized in the look up Table 2. The first column in this table is designated as FLAG parameter formulated specifically in the present study that takes on the values from 1 to 24, 0 and 100, which govern all the decision rules summarized in the remaining columns.

For instance, when FLAG = 20 the decision logic rule is: **IF** there is one positive peak in the R-R interval ($RR_t$), its position w.r.t. the midpoint of the interval is towards the right, the consecutive R peaks ($R_1$ and $R_2$) being +ve in the interval, S peaks ($S_1$ and $S_2$) having a magnitude greater than 0.24 mV w.r.t. base level, and heart rate (HR) greater than 118 bpm; **THEN**, this peak represents a T wave.

**Diagnostic Features Extracted/Deduced from ECG Signal**

The 37 useful diagnostic features that have been extracted /deduced for arrhythmia detection using the above methodology are as follows:

**Features Extracted from QRS Complex**

R peak sample number, R peak amplitude (mV), R peak angle, Q peak sample number, Q peak amplitude (mV), S peak sample number, S peak amplitude (mV), S peak angle, R′ peak sample number, R′ peak amplitude (mV), QRS onset, QRS onset amplitude, QRS offset, and QRS offset amplitude are extracted from QRS complex

**Features Deduced from QRS Complex**

QRS width, R-R interval, Heart rate (bpm), VAT (ventricular activation time), amplitudes of Q, R, R′ and S peaks w.r.t. QRS onset, amplitude of QRS offset w.r.t. amplitude of QRS onset for a given QRS complex, QRS configuration (Table 1) are determined from the extracted features of the QRS complex.

**Features Extracted from R-R interval**

Detection of isoelectric line between two consecutive QRS complexes in the R-R interval, presence of P/T waves, polarity (+/-) of P/T waves, and position of P/T waves w.r.t. mid-point of R-R interval are the extracted features from R-R interval. All these features are represented by a parameter termed as 'FLAG', which is assigned integer values (+ve) that indicate the presence, polarity, position and number of P/T waves in an R-R interval w.r.t. isoelectric line detected between two consecutive QRS complexes and w.r.t. mid-point of R-R interval.

**Features Extracted in R-R interval from P wave**

P peak sample number, P peak amplitude (mV), P wave onset, P wave offset, P wave onset amplitude (mV), and P wave offset amplitude (mV) are the extracted features in R-R interval from P wave

**Features Deduced from R-R intervals**

P-R intervals, P-R segments, P-P intervals, amplitude of P peak w.r.t. its onset, amplitude of P wave offset w.r.t amplitude of P wave onset for a given P wave, and AVCR (Atrio-Ventricular Conduction Ratio) are deduced from R-R interval parameters.

**EVALUATION OF DEVELOPED METHOD USING SIMULATED SIGNALS**

The algorithms developed for the detection of QRS complex and its associated parameters, and for the detection of P wave and its associated features,

described above, have first been tested using simulated ECG signals. Testing any algorithm by applying it to a simulated signal helps to create an approximate software scheme, which when used for real time data analysis aids in the selection of optimised values of different parameters related to the logic and sequence of data interpretation.

Keeping this in mind, artificial ECG signals, sampled at 360 Hz, have been simulated for a number of abnormal beats and rhythms, as per the requirement of an arrhythmia type regarding the relative locations and amplitudes of the P waves and the QRS complexes. Signals that have been simulated conform to the morphological variations present in the MLII ECGs of the MIT/BIH arrhythmia database.

While the simulated ECG signals were designed and analysed to test the algorithms for feature extraction, a number of detailed calculations had to be carried out to adjust the tolerance limits and threshold criteria for the 37 useful diagnostic features listed in Section 3.2.

After the simulated data test runs were conducted, a set of algorithms was obtained which provided a powerful, dynamic and automated ECG analysis model that was subsequently validated by the real-time ECGs acquired from standard data.

## VALIDATION OF DEVELOPED METHOD USING STANDARD ECG DATA

### Validation using CSE Data

If an algorithm detects ECG features within the tolerance limits prescribed by the CSE group [39], then the influence of errors in measurement of ECG parameters by the algorithm does not affect the diagnostic significance of these parameters.

To facilitate the validation of an ECG analysis algorithm, 25 records containing 8-10 s of 15 lead ECG data sampled at 500 Hz have been provided with measurement results and recommended tolerances for P onset, P offset, QRS onset, QRS offset and T end in CSE Data Set-3 [34,39].

For lead II, the recommended tolerance for P onset is 8.0 ms, P offset is 12.8 ms, QRS onset is 7.8 ms, and QRS offset is 12.4 ms. In terms of samples, these tolerances are 4.0, 6.4, 3.9 and 6.2 respectively, for CSE records sampled at 500 Hz, and, 2.88, 4.608, 2.808 and 4.464 respectively for the MIT/BIH records sampled at 360 Hz.

In view of the above, the QRS detection algorithm to detect R peak (location) as the QRS fiducial, was validated using all the 25 records for lead II of the CSE Dataset-3. Lead II ECG signals were specifically chosen, since the algorithms in the present study have been used to analyse modified lead II ECGs of the MIT/BIH data, for arrhythmia analysis.

The performance of the algorithm for QRS detection in terms of R peak fiducial was found to be satisfactory for all the 25 records (record nos. 1, 6, 11, 16, 21, 26, 31, 36, 41, 46, 51, 56, 61, 66, 71, 76, 81, 86, 91, 96, 101, 106, 111, 116 and 121), and all the QRS complexes were detected successfully.

The composite method of feature extraction was also validated for computational accuracy of P onset, P offset, QRS onset and QRS offset using lead II ECG signals of records 16, 21, 31, 66, 96, 101 and 106 of Data Set-3. The numerical values of these four parameters, computed by the software developed, were found to be within the recommended tolerances for all the 85 beats present in these 7 records.

Using the measurement results of 85 beats present in the 7 records, the computed values for R peak amplitudes (w.r.t. the baselevel), R-R interval, FLAG parameter, P-R interval, P-R segment, P-P interval, and AVCR were also validated.

### Validation using MIT/BIH Data

The process of validation was further carried out for the detection of QRS complexes, in terms of R peak fiducials from the annotated records of the MIT/BIH database. All the records are annotated at R peak points, and hence provide true locations of QRS complexes.

The QRS detection algorithm was validated using 32,800 beats acquired from records 100, 101, 103, 105, 109, 113, 114, 116, 209, 213, 214, 219, 231, 232, and 234. Except 14 false detections (9 false positive and 5 false negative), 32,786 beats were detected correctly, wherein 7, 21, 292 QRS features out of 721,600 extracted QRS features were found to be correct and a detection accuracy of 99.96% within the tolerance limits recommended by the CSE Working Party. The QRS complexes detected as false positive were isolated QRS-like artifacts.

Too much tilt in an IE line is undesirable as it leads to erroneous detection of P and T peaks. The amplitude band defined for identification of R peak point has a special significance in this context (refer to Fig. 4). It decides the range in which the R peak amplitudes lie in

the ECG signals with a baseline wander from 0.05 to 0.25 Hz. Due to this band, the IE line computed in an R-R interval has a limited tilt that does not effect the detection of P and T peaks. Starting from the P peak point determined w.r.t. the IE line, P onset and P offset are detected using the slope criteria only for the filtered signals.

Therefore, tilted IE lines do not influence their computations, and therefore, these P wave boundaries are detected within the recommended tolerances given by the CSE Working Party. These computations were verified manually by observation of the plots of the signal under analysis. The actual P peak amplitude is computed w.r.t. P onset, which is taken as the base level for all P wave measurements. In cases of serious baseline wander, to compute P waves and their parameters in the time domain, techniques for suppression or removal of baseline wander need to be employed.

Authors in [18] have reported that onsets and offsets of P and T waves may not have accuracy essential for diagnostics when these are influenced by heavy noise or baseline wander or when their magnitudes are very small.

The present method is effective for most of the records of the MIT/BIH database that are contaminated by noise within acceptable levels. Very noisy signals are exceptional data segments and in the authors' knowledge have been known to create difficulty for other techniques of ECG analysis as well. As also pointed out by Gang et al. [20], reliability of any technique may not be judged only on the basis of its ability to analyse very noisy signals.

**Performance Evaluation of the Composite Method**

The composite method of feature extraction was applied to detect R peaks, QRS features like QRS onset, QRS offset, QRS width etc., IE line, P/T peaks in an R-R interval and P wave features like P onset, P offset, P wave magnitude etc. from 8000 beats of records 100, 101, 103 and 219. Consistency in the values of FLAG parameter was also assessed using these beats.

The software extracted all the 37 features to an accuracy that was well within the recommended tolerance limits. Verification of the results obtained by the method was performed on the basis of detailed manual measurements of the ECG plots constituted by 8000 beats: 2200 beats of record 100, 1800 beats of record 101, 2000 beats of record 103, and 2000 beats of record 219 of the MIT/BIH database that were successfully identified as QRS complexes by the software.

An unclassifiable beat in a data segment of Record 101 was detected as QS wave. Varying morphology of the QRS complexes in record 219 did not pose any problems in the satisfactory detection of QRS features. Presence of undulations as fibrillatory waves was also identified in the rhythms of this record.

The abnormal QRS complexes in this record have large amplitudes but have slopes that do not fall within 55% of the highest slope of a rising R wave (slope threshold criteria for QRS detection) in the rhythm under analysis (2500 sample points are analysed at a time). To detect these complexes, a suitable width criteria (if the QRS width is less than or equal to 1.5 times the stipulated maximum width of normal QRS complexes then the tentative R peak is marked as a valid QRS complex) was employed that also discriminate these large complexes from comparable T waves.

After the extensive process of testing and validation of the composite method of feature extraction over a considerably large amount of standard ECG data the software was applied again to extract all the 37 features from each of the 12 s pathological data segments of records 100, 119, 201, 202, 205, 209, 219, 232 and 233 (approx. 250 beats). These ECG signals were not used earlier for analysis. Various characteristics found in these data segments are as follows:

Normal Rhythm, record 100; Ventricular bigeminy (with uniform PVCs having +ve R wave), Ventricular trigeminy (with uniform PVCs having +ve R wave), record 119; Pure atrial fibrillation, record 201; Sinus bradycardia, record 202; R-on-T premature ventricular complex, Slow ventricular tachycardia, record 205; Supra-ventricular tachycardia, record 209; Atrial fibrillation + premature ventricular complex + T wave, record 219; Sinus bradycardia + right bundle branch block + A-V block I, record 232; and, Isolated premature ventricular complex (QS wave) + atrial premature complex, Isolated premature ventricular complex with prominent S peak (+ve R wave), record 233.

**Discussion on Results**

In all the 12 s pathological recordings, a large variation is present in the morphology of the QRS complexes. Also the P and T waves have different magnitudes and polarities in these signals. The signals were analysed with noise within acceptable levels and a baseline drift

in the range from 0.05 Hz to 0.25 Hz. All the 37 features were successfully detected in these signals with 100% accuracy, i.e. the accuracy of detection was satisfactory enough to classify these parameters into different diagnostic categories.

Once the correct value of the FLAG parameter was identified by the program, computation of P wave features was relatively easy. Width of the QRS complex is widely used to identify premature ventricular complexes, and its correct determination has also been of much significance.

The maximum value of QRS width for practically all normal QRS complexes detected in the signals was found to be 0.115 s, although its upper limit has been specified as 0.12 s in general, and 0.10 s, 0.11 s in particular [1-3].

Some wide and abnormal QRS complexes were found to have their widths as low as 0.117 s. In record 202, the width of few normal QRS complexes was found to be 0.122 s. However, to detect bradycardia in record 202, the QRS width criteria is not required (heart rate computations are sufficient), and in general the maximum limit of normal QRS width was fixed at 0.115 s.

Since the signals subjected to analysis have been shifted upwards by the baseline (0 mV), to obtain only positive amplitudes of ECG waves, all the amplitudes have been initially computed from this shifted baseline. Subsequently, the exact amplitudes of QRS wave were computed w.r.t. to the QRS onset as the base level while those of P wave were computed w.r.t. P onset as the base level.

More than 8250 R-R intervals were filtered and analysed in a number of normal and abnormal rhythms of the MIT/BIH database. During this process of validation, the extracted/deduced features were measured in the filtered signals and manually verified against those in the unfiltered ECGs. The results of two representative abnormal rhythms for MIT/BIH Rec. No. 205 with signal duration 1677.989 – 1684.3 s, and, MIT/BIH Rec. No. 202 with signal duration 1107.333 – 1113.997 s, are shown in Figs. 8-9, Tables 3-4 and Figs. 10-11, Tables 5-6, respectively.

The length of the data segments shown has been restricted due to limitation of space. Figures 8-9 and 10-11 show the unfiltered signal and the signal with filtered non-QRS portions for Rec. Nos. 205 and 202, respectively. Tables 3-6 present the entire features extracted /deduced i.e., features pertaining to QRS wave and R-R interval (refer Sec. IIIB), for the above two records (for symbols used in Tables 3-6, refer Table 7). For example, Table 3 gives the 22 features extracted/deduced pertaining to each of the 9 QRS waves present in the signal duration 1677.989 – 1684.3 s of Rec. No. 205, while Table 4 gives the 15 features extracted/deduced pertaining to each of the 8 R-R intervals present in the above record.

The automated extraction of diagnostic features, using the composite methodology, can be employed by a suitable classifier such as a knowledge-based expert system for easy and reliable interpretation of single as well as multiple arrhythmic events in an ECG signal. For example, using the above extracted features in the knowledge-base of an expert system, it can be reliably interpreted that in Rec. No. 205, the $7^{th}$ QRS wave shows isolated R-on-T Premature Ventricular Complex (PVC) with downright R peak, and the interval between $7^{th}$ and $8^{th}$ R peaks shows Full Compensatory Pause (FCP).

## ADVANTAGEOUS FEATURES OF THE DEVELOPED METHODOLOGY

A number of computer-based techniques are reported in literature for feature extraction of ECG signals. As the QRS complex is more distinguishable and easier to detect in comparison with other ECG waves, the R-peak point is generally used as a reference to reliably detect the QRS wave; on the basis of QRS detection, other prominent features are extracted from the ECG signal [6, 47].

Various methods developed so far for detection of QRS complex can be broadly classified into four categories, viz., syntactic methods, non-syntactic methods, transformative methods and hybrid methods [26, 36, 47-49].

The diversity of algorithms developed for QRS detection and extraction of the P wave, is too large to compare with the algorithms developed in the present study for detection of the QRS and P waves. Therefore, the comparison has mainly been restricted to distinctive QRS complex and P wave detection methods, applied to signals of the MIT/BIH database.

Pan and Tompkins [13] developed a real-time QRS detection algorithm to reliably recognize QRS complexes based upon analyses of slope, amplitude, and width. Hamilton and Tompkins [14] implemented another real-time QRS detection algorithm using a preprocessor stage to produce event vectors consisting of peak heights and time of peak occurrence, on the basis of the previous method [13], from the processed ECG signal.

In the next stage of ECG processing, complex decision rules were applied progressively to these event vectors to evaluate the quantitative results of various decision rule components. In both the methods, P wave detection has not been addressed.

Similarly, Lin and Chang [7] used linear prediction for QRS feature extraction only. Xue et al. [15] developed a multilayered neural network based adaptive matched filter to detect QRS complexes from ECG signals. The technique does not report the diagnostic value of detected QRS complexes regarding different arrhythmias in context to differing morphologies.

Murthy and Prasad [16] developed a pole-zero models to measure P, QRS and T waves. However, no method has been given to distinguish a P wave from a T wave in real-time ECG signals.

Woolfson [8] applied Kalman filtering to short stretches of ECG data for computing the time varying spectra of the R-R intervals. Variations in the morphology of the QRS complex and detection of the P wave, two important parameters necessarily needed to interpret arrhythmias, have not been addressed in this study.

Poli et al. [17] used genetic algorithms to detect QRS complexes in the ECG signals of the MIT/BIH database. However, the diagnostic importance of the detected QRS complexes has not been mentioned in the study. Li et al. [18] used an algorithm based on the wavelet transform to first detect the QRS complex, then the T wave, and finally the P wave from single channel records.

As, acknowledged by the authors, onsets and offsets of P and T waves were not detected to an accuracy required for reliable arrhythmia interpretation. Sahambi et al. [12] used wavelet transform to obtain multiscale analysis for timing characterization of the ECG, for detecting the QRS complex, and, P and T waves with positive and negative polarity. The study has presented the results only for record 106 of the database.

Wieben et al. [9] used the concept of filter bank to implement time-frequency analysis of MLII ECG records. The authors also analysed these ECG signals to obtain heart rate and QRS morphological features. The filter bank features, and the heart rate and QRS features were used to classify only premature ventricular complexes.

Gang et al. [20] used linear-approximation distance-thresholding compression with a backpropagation neural network to detect normal and abnormal QRS complexes from eight records of the MIT/BIH database. However, the method has not been used to detect P and T waves in these ECG signals. Bartolo et al. [10] have developed QRS detection software based on QRS template matching process.

Record segments with poor signal quality, where most of the QRS complexes were visually indistinguishable from background activity, were excluded from analysis. As suggested by the authors, further improvement in discriminating normal and abnormal premature beats required detection and analysis of the P wave that was not attempted in the study.

Osowski and Linh [11] statistically transformed QRS complex to obtain a suitable feature vector. The feature extraction method does not detect the P wave that is of utmost importance to classify arrhythmias. Botter et al. [19] used a backward-error-propagation neural network with asymmetric basis functions to extract the features of P waves as a set of nine parameters.

The method does not address detection of the QRS complex, in the absence of which arrhythmias can hardly be classified, except the atrial fibrillation and the atrial flutter rhythms. Owis et al. [21] presented a study of the non-linear dynamics of ECG signals for arrhythmia characterization. The results indicated that the discrimination between different arrhythmia types is difficult using features obtained by this study.

Shyu et al. [22] used quadratic spline wavelets to detect QRS complexes from seven records of the MIT/BIH database. P wave detection has not been addressed in the study. Chazal et al. [23] presented automatic classification of heart beats using ECG morphology and heart beat interval features. In this work, QRS fiducials provided by the standard annotations have been directly utilized to obtain different ECG features.

R peak detection has not been performed. Illanes-Manriquez and Zhang [49] detected QRS onset and offset in ECG signals by computing an indicator related to the area covered by the QRS complex envelope. However, P wave detection was not addressed in the study.

On comparing the composite method, developed in the present study, with the methods used by other researchers discussed above to detect QRS and P waves from ECG signals of the MIT/BIH database, four unique contributions of the developed composite method emerge:

- Extraction of QRS complexes in such a way that their original morphology is preserved for accurate

IJBST

ISSN: 0974 – 3987
IJBST (2009), 2(7): 96-125

determination of several features of diagnostic importance, and detection of P waves in a manner that these can be well discriminated from T waves in different abnormal rhythms;

- Demonstration of the inherent strength of the method for signal classification that is not so transparent in other known techniques applied to the analysis of a variety of real-time normal and abnormal beats and rhythms; providing an amenable technique that can be appreciated and modified by a cardiologist;
- A simple and understandable technique (devoid of any 'black-box' effect) that is more practical in a clinical environment, and provides a powerful medical information processing system that can be successfully employed to train medical personnel responsible for ECG waveform delineation;

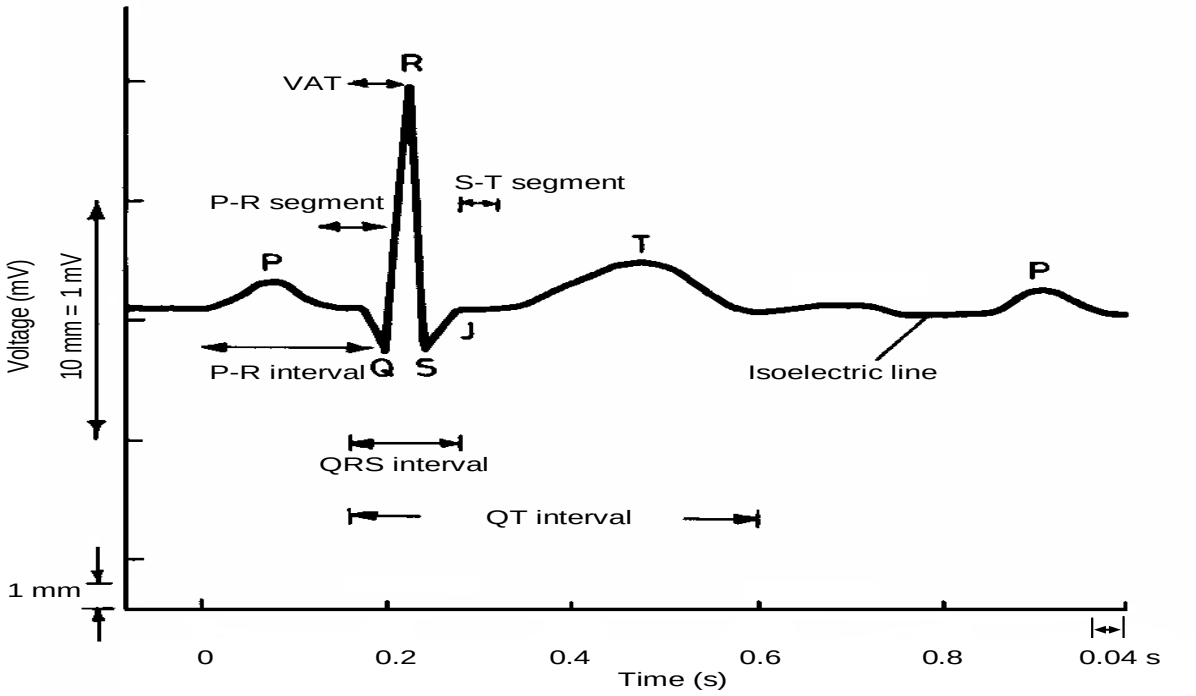


**Fig. 1. Normal ECG cardiac cycle**

IJBST

ISSN: 0974 – 3987
IJBST (2009), 2(7): 96-125

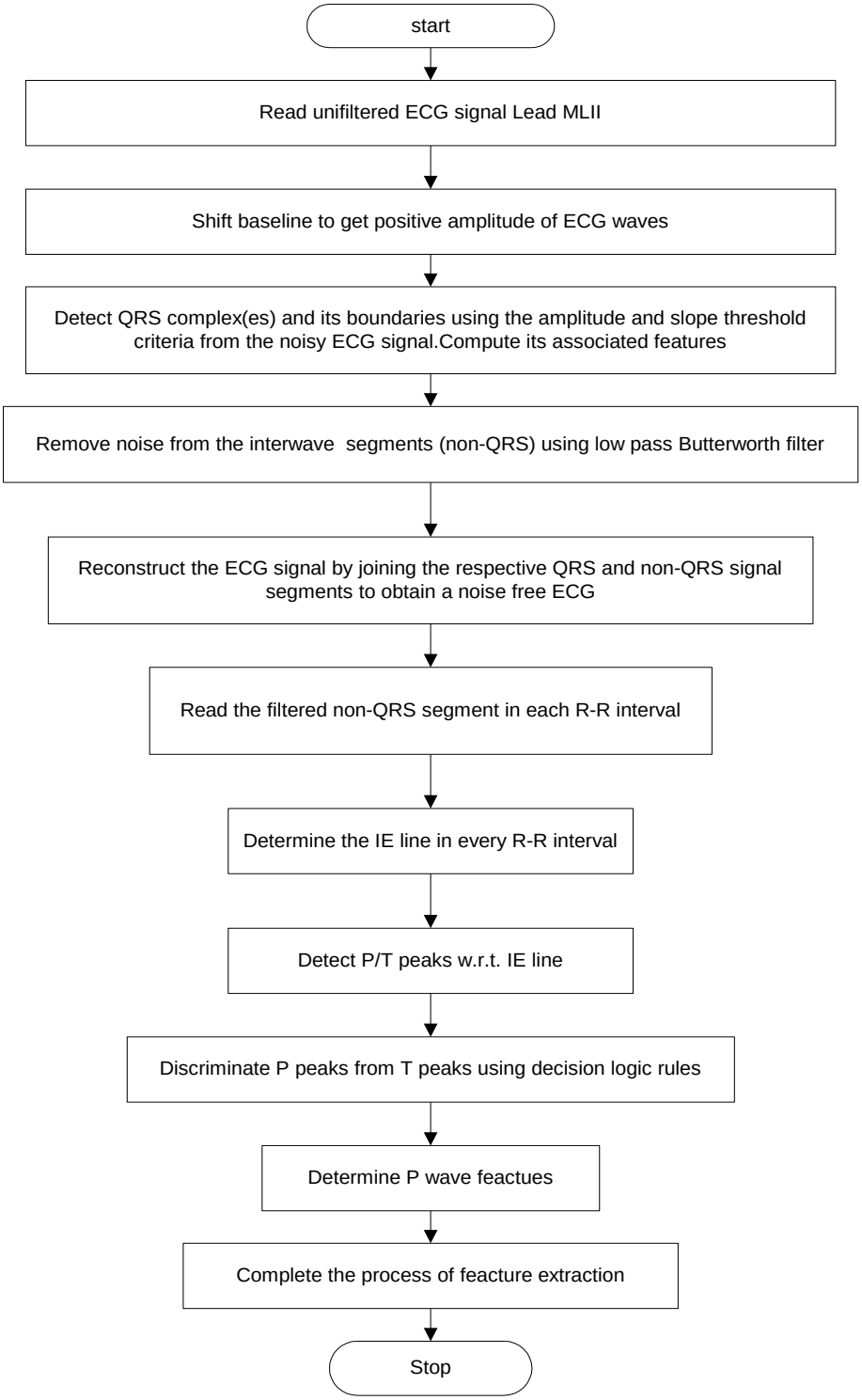


**Fig. 2. Flow diagram depicting the steps followed in the composite method of feature extraction**

IJBST

ISSN: 0974 – 3987
IJBST (2009), 2(7): 96-125

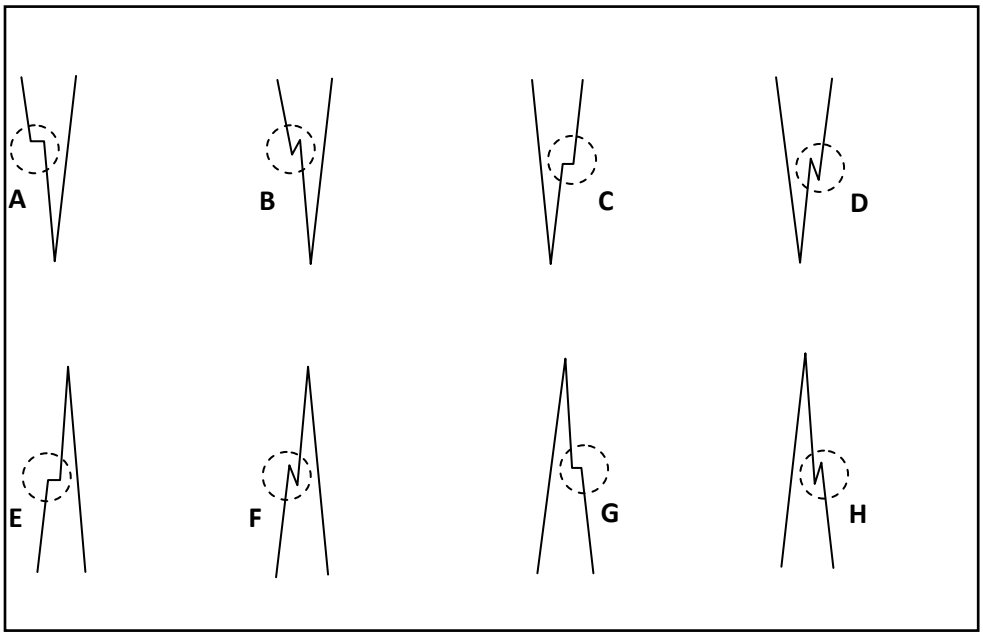


**Fig. 3. Slurs (A, C, E, G) and notches (B, D, F, H) in component waves (Q-R-S-R′) of the QRS complex**

IJBST

ISSN: 0974 – 3987
IJBST (2009), 2(7): 96-125

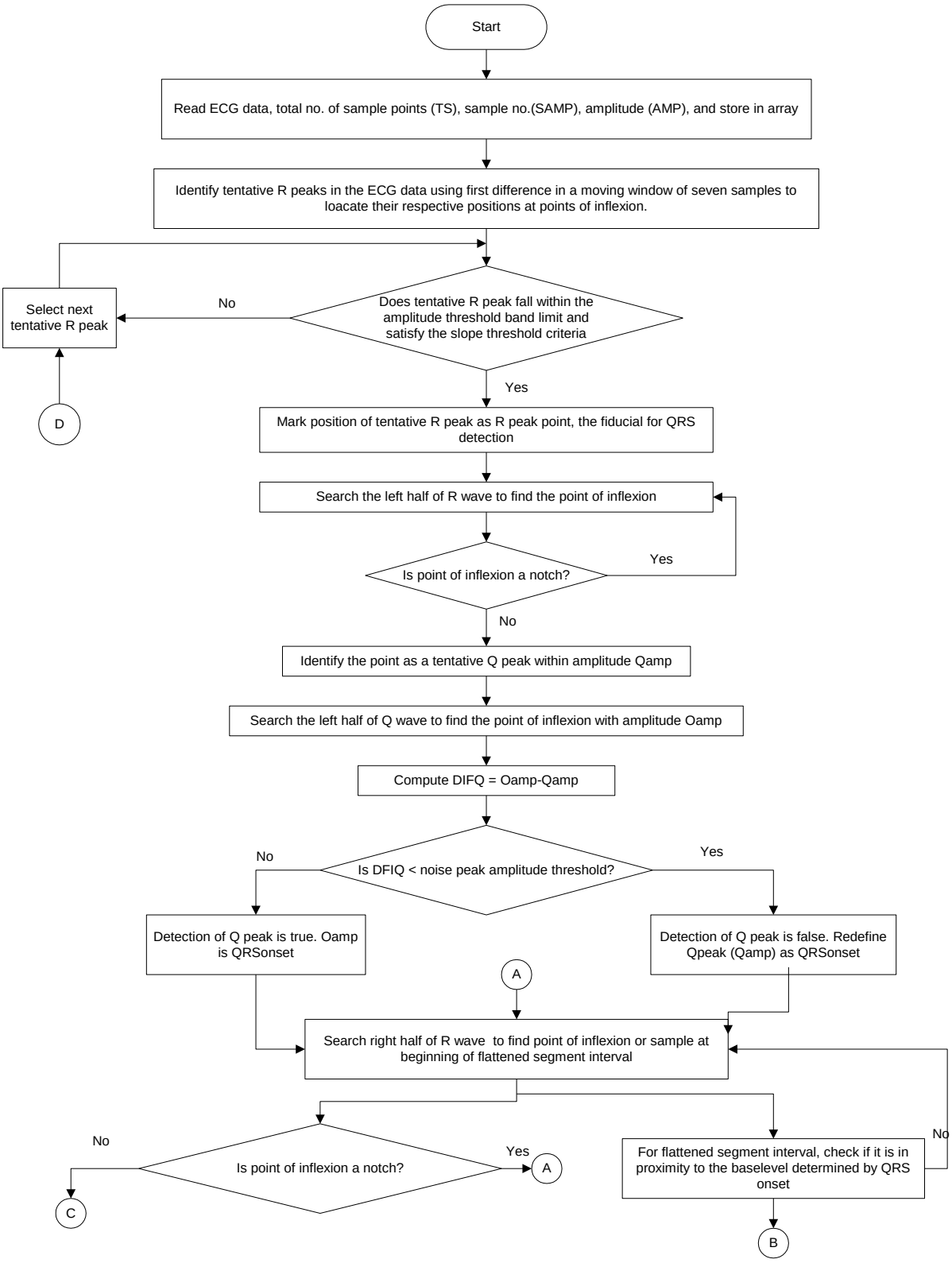


**Fig. 4. Flowchart for recognition of QRS wave and characteristic point identification**

ISSN: 0974 – 3987
IJBST (2009), 2(7): 96-125

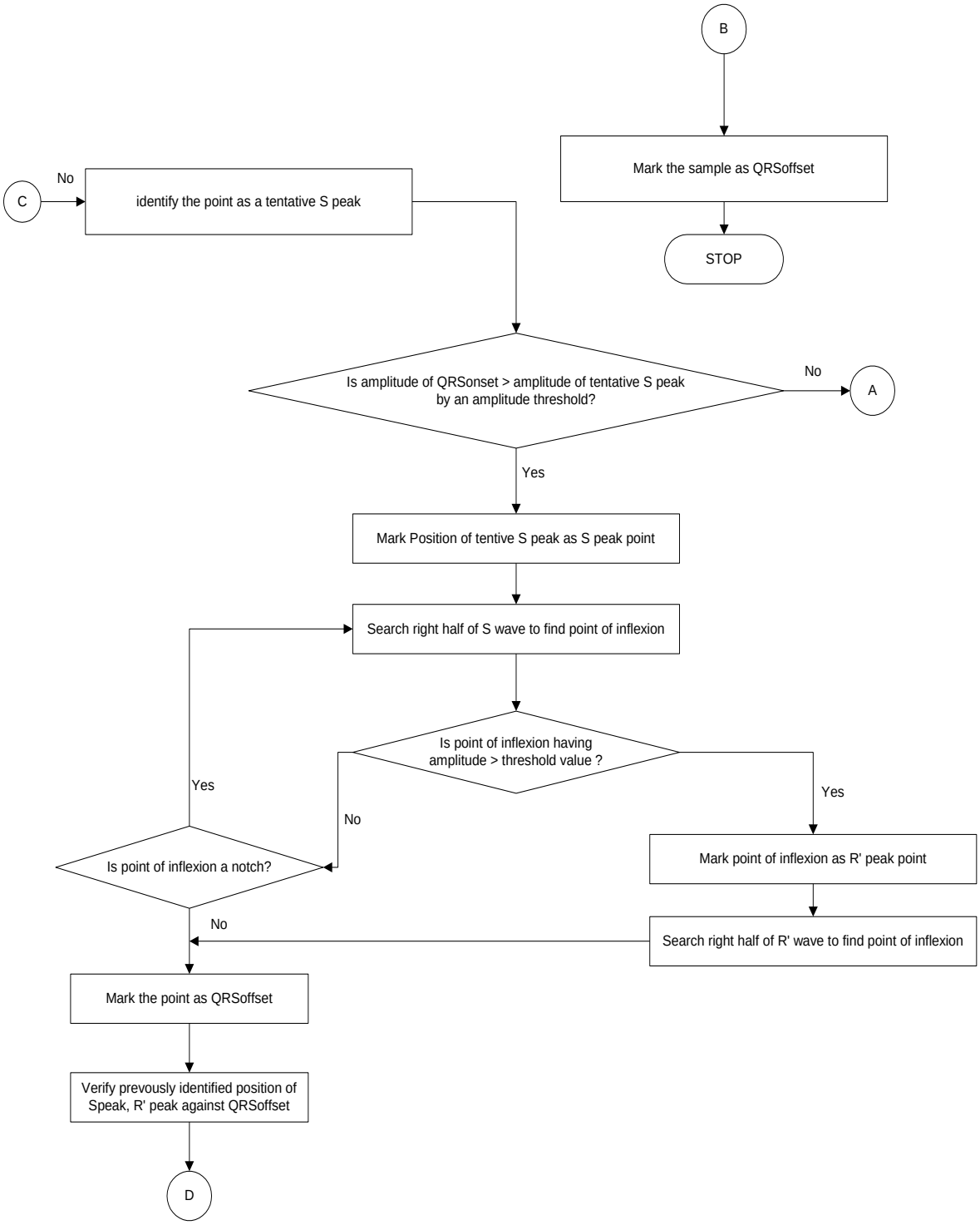


**Fig. 4. (cont.)**

IJBST

ISSN: 0974 – 3987
IJBST (2009), 2(7): 96-125

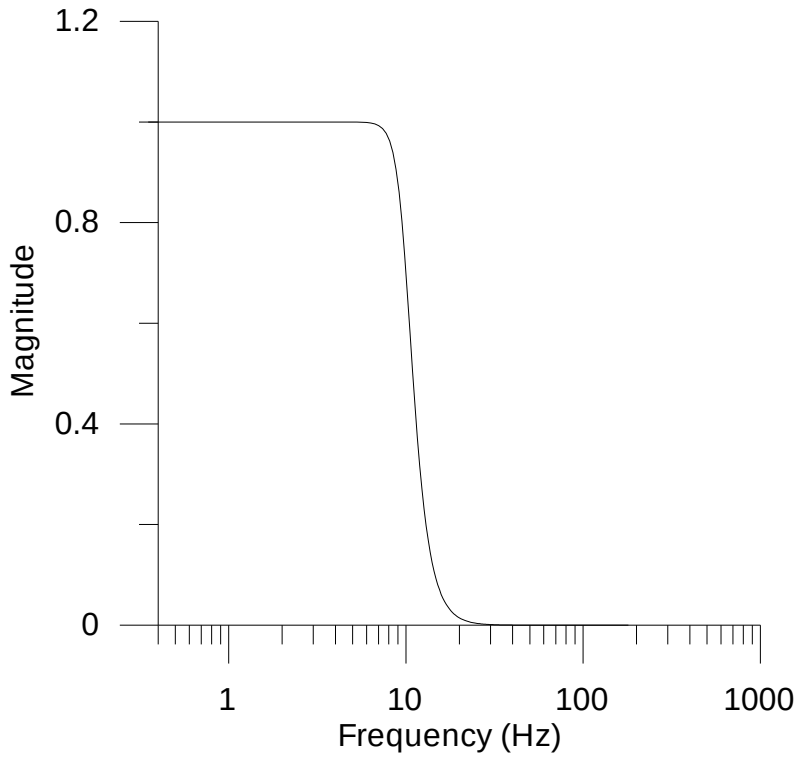


**Fig. 5. Amplitude responses of 6th order low pass Butterworth Filter with cut off frequency of 10 Hz**

IJBST

ISSN: 0974 – 3987
IJBST (2009), 2(7): 96-125

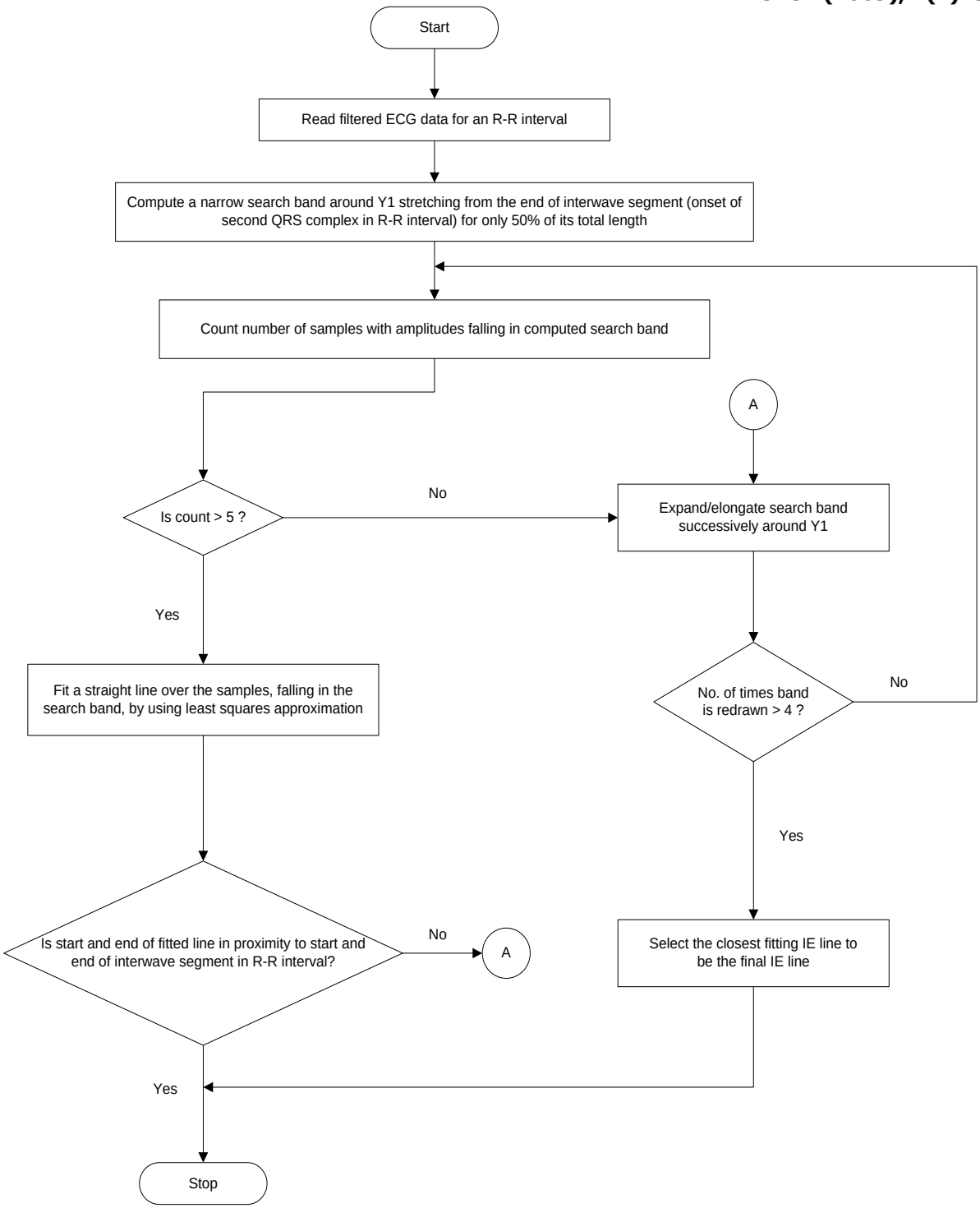


**Fig. 6. Flow chart for detection of IE line**

IJBST

ISSN: 0974 – 3987
IJBST (2009), 2(7): 96-125

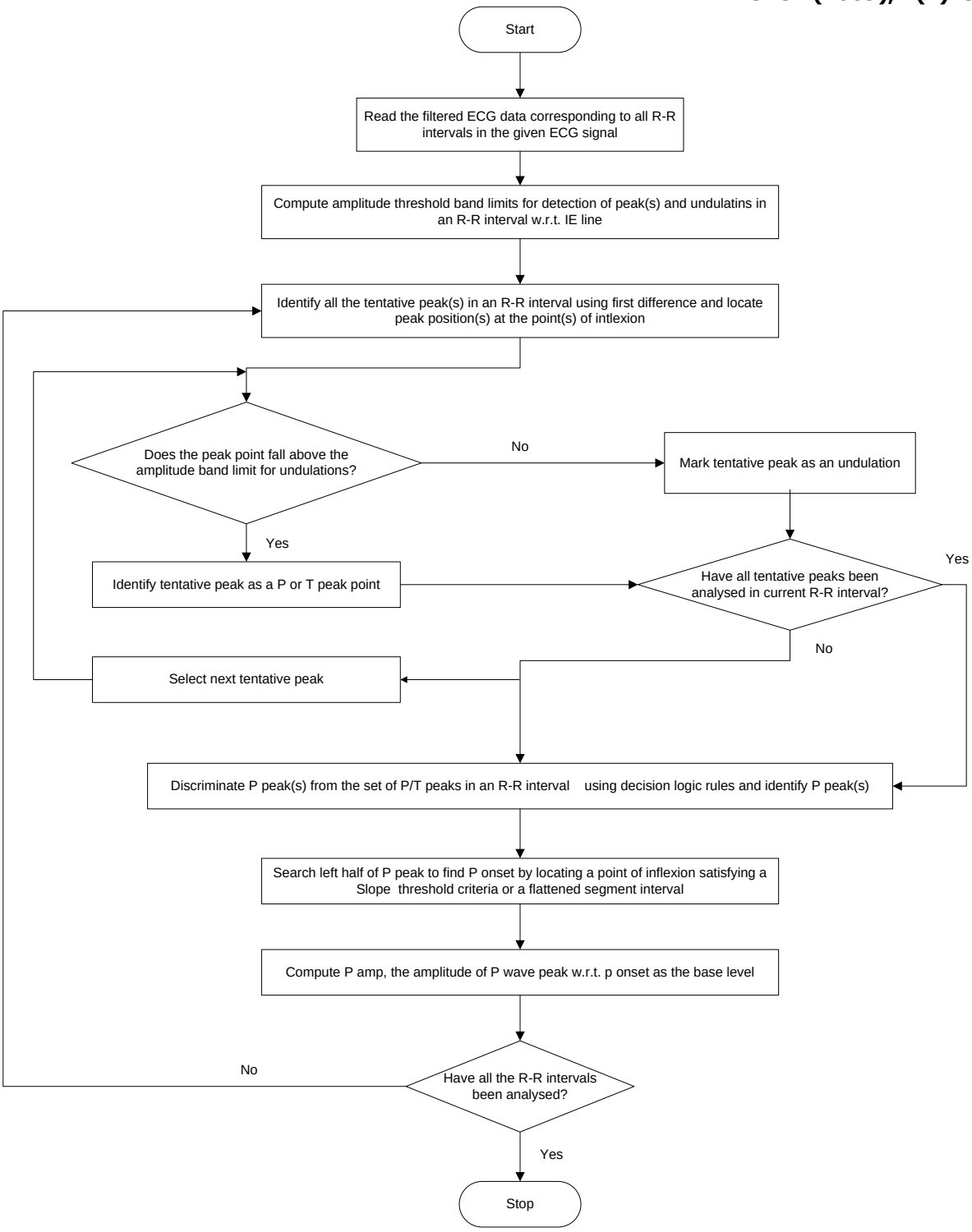


**Fig. 7. Flow chart for recognition of P wave and characteristic point identification**

IJBST

ISSN: 0974 – 3987
IJBST (2009), 2(7): 96-125

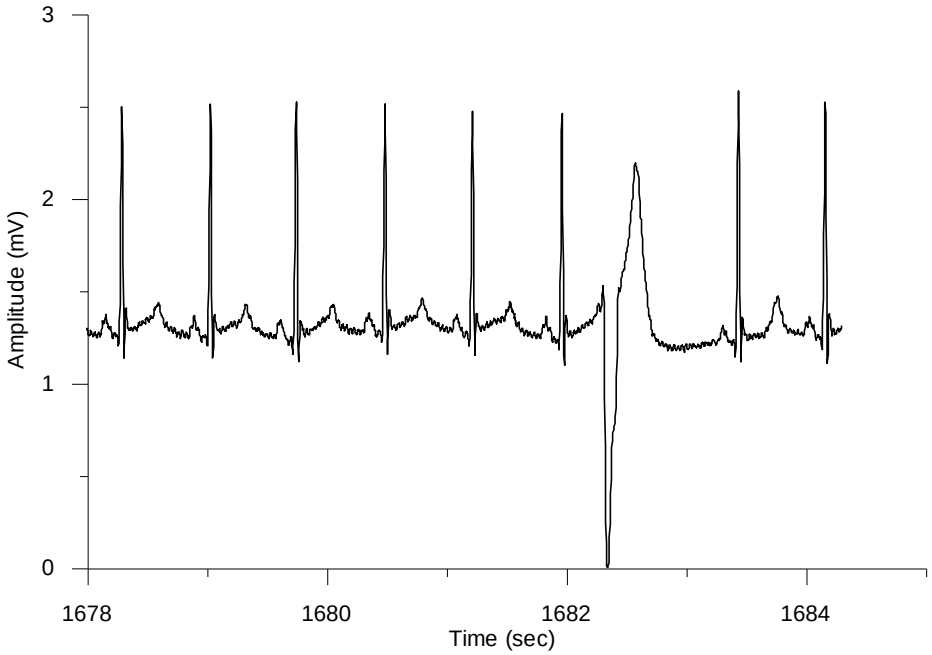


**Fig. 8. Unfiltered MLII signal (MIT/BIH Rec. No. 205)**

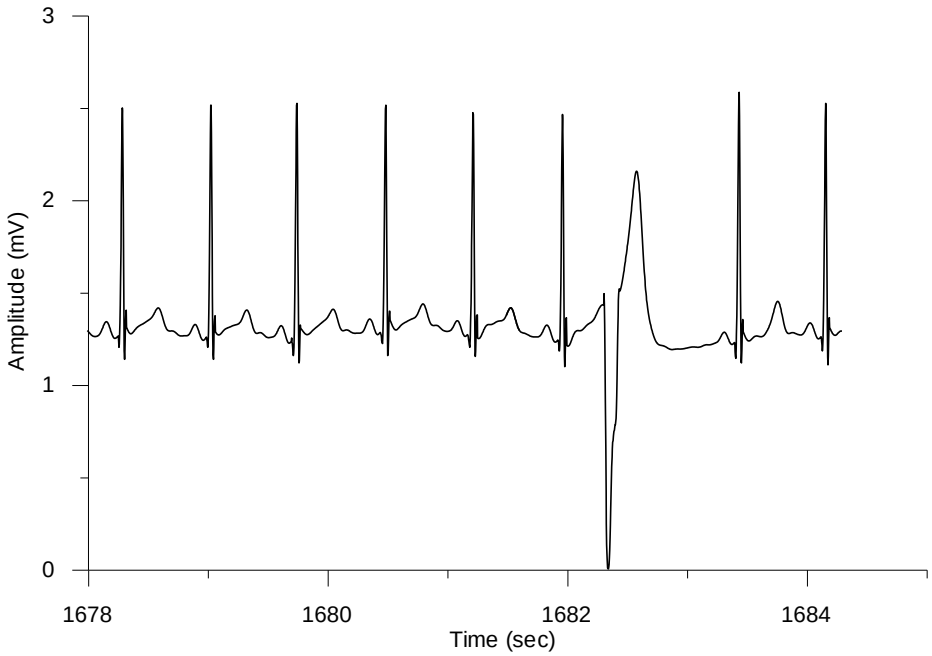


**Fig. 9. MLII signal with filtered non-QRS portions (MIT/BIH Rec. No. 205)**

IJBST

ISSN: 0974 – 3987
IJBST (2009), 2(7): 96-125

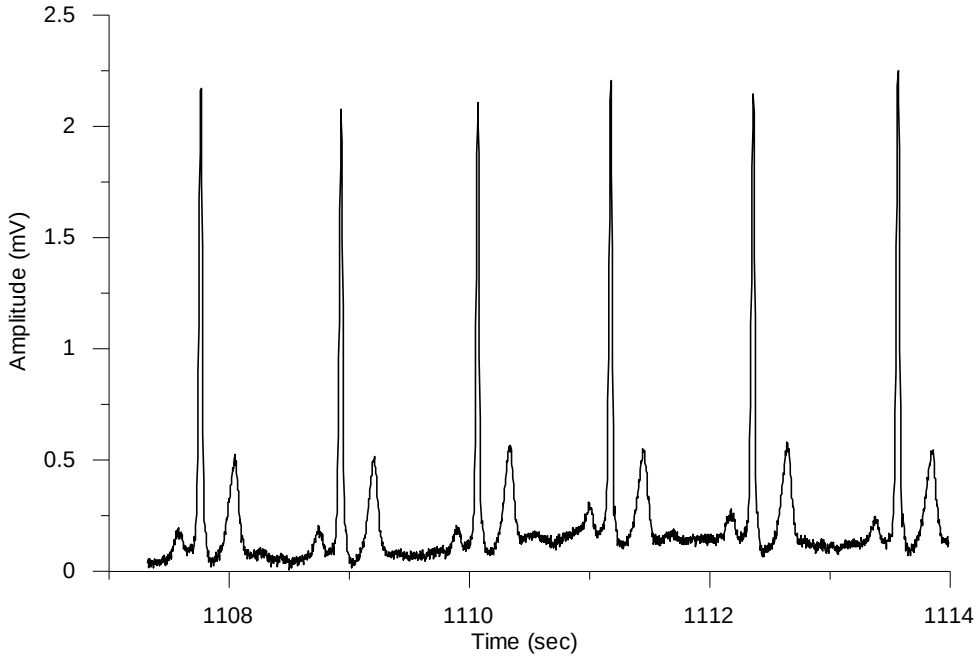


Fig. 7 Unfiltered MLII signal (MIT/BIH Rec. 202)

**Fig. 10. Unfiltered MLII signal (MIT/BIH Rec. No. 202)**

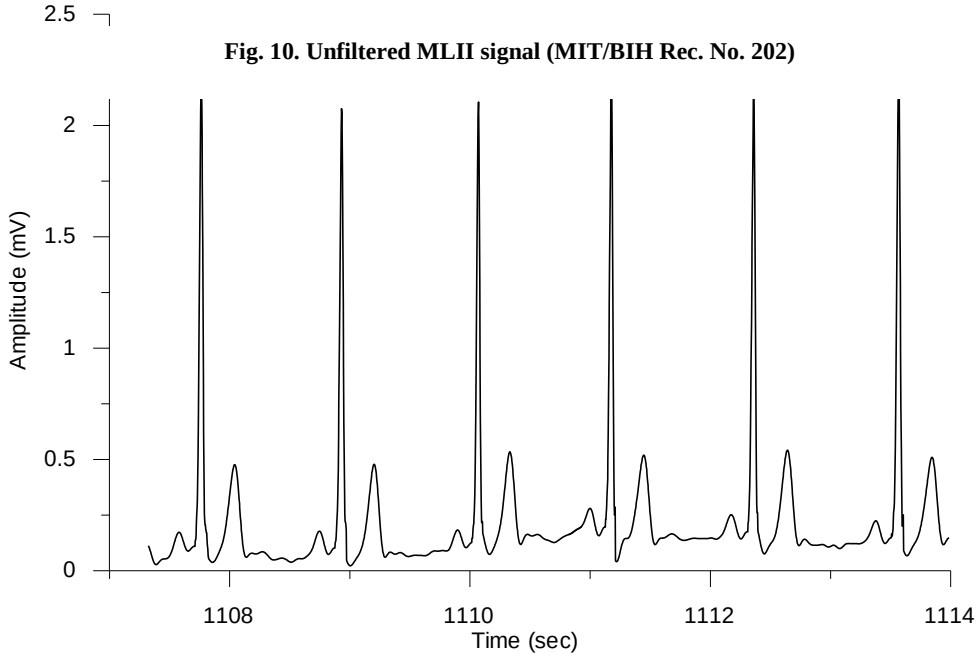


Fig. 8 MLII signal with filtered non-QRS portions (MIT/BIH Rec. 202)

IJBST

ISSN: 0974 – 3987
IJBST (2009), 2(7): 96-125

Table 1 Different configurations of the QRS complex (MLII)

| QRS morphology | Configuration designation |
|---|---|
| 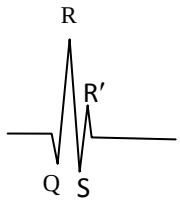  | QRSR′ |
| 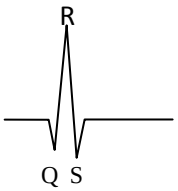  | QRS |
| 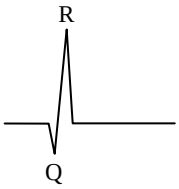  | QR |
| 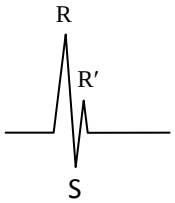  | RSR′ |
| 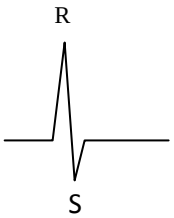  | RS |
| 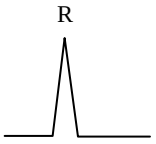  | R |
|  Single negative peak (R wave absent) | QS |

IJBST

ISSN: 0974 – 3987
IJBST (2009), 2(7): 96-125

Table 2. Look-up table of decision logic rules developed for discriminating between P and T peaks/waves in an R-R interval

| FLAG | No. of peaks present in R-R interval | Polarity (+ve/-ve) of peaks in R-R interval ($RR_t$)* | | | Position of peaks with respect to midpoint in R-R interval (L, M, R)* | | | Additional criteria to determine peak/wave type (P or T) in R-R interval ($RR_t$)* | Discrimination of peak/wave type (P or T) present in R-R interval | | |
|---|---|---|---|---|---|---|---|---|---|---|---|
| | | 1st peak | 2nd peak | 3rd peak | 1st peak | 2nd peak | 3rd peak | | 1st peak | 2nd peak | 3rd peak |
| 1 | 2 | +ve | +ve | - | L | R | - | HR = 60-100 bpm in $RR_t$ | T | P | - |
| 2 | 1 | +ve | - | - | L/M | - | - | HR>118 bpm in $RR_t$; $RR_t$ with +ve $R_1$ & +ve $R_2$ both with S waves | T | - | - |
| 3 | 2 | -ve | +ve | - | L | L | - | - | P | T | - |
| 4 | 2 | +ve | +ve | - | L | L | - | - | T | P | - |
| 5 | 2 | -ve | +ve | - | L | R | - | HR>118 bpm in $RR_t$; $RR_t$ with +ve $R_1$ & +ve $R_2$ both with S waves | P | T | - |
| 6 | 1 | +ve | - | - | R/M | - | - | HR = 60-100 bpm in $RR_t$; $RR_t$ with +ve $R_1$ & +ve $R_2$ | P | - | - |
| 7 | 1 | -ve | | - | L | - | - | $RR_t$ with +ve $R_1$, $R_2$ | T with undulations after it | | |
| 8 | 1 | +ve | - | - | L/M | | | $RR_t$ with -ve $R_1$ & -ve $R_2$ & no S waves | T | - | - |
| 9 | 2 | -ve | +ve | | L | R | | - | T | P | - |
| 10 | 3 | -ve | +ve | +ve | L | L | R | $RR_t$ with +ve $R_1$, $R_2$; $S_1$, $S_2$ > 0.24 mV | P | T | P |
| 11 | 1 | +ve/-ve | - | - | M/R | - | - | $RR_t$<($RR_{t-1}$ or $RR_{t+1}$) | T | - | - |
| 12 | 1 | -ve | - | - | R | - | - | Peak amplitude >= half the amplitude of higher R peak in $RR_t$ | T | - | - |
| 13 | 1 | +ve | | | R | | | HR = 60-100 bpm in $RR_t$ | P with undulations before it | | |
| 14 | 3 | -ve | +ve | +ve | L | L/M | R | HR = 60-100 bpm in $RR_t$ | Di-phasic T | | P |
| 15 | 2 | +ve/-ve | +ve/-ve | | L/M/R | L/M/R | | Peaks are extremums of sawtooth waves | P/flutter wave | P/flutter wave | - |
| 16 | 3 or more | +ve | +ve | +ve | L/M/R | L/M/R | L/M/R | HR < 120 bpm in $RR_t$; $S_1$, $S_2$ < 0.24 mVor absent in $RR_t$ | All the peaks are P peaks | | |

Int

* L: left of mid-point; M: at mid-point; R: right of mid-point of R-R interval; QRS(W): width of QRS complex; $RR_t$: interval (in sec) between two consecutive R peaks, say $R_1$ & $R_2$; $RR_{t-1}$: R-R interval preceding $RR_t$; $RR_{t+1}$: R-R interval succeeding $RR_t$; HR : heart rate in bpm; '-' symbolizes absence of respective peak/ wave in corresponding R-R interval.

(contd…)

IJBST

ISSN: 0974 – 3987
IJBST (2009), 2(7): 96-125

| FLAG | No. of peaks present in R-R interval | Polarity (+ve/-ve) of peaks in R-R interval ($RR_t$)* | | | Position of peaks with respect to midpoint in R-R interval (L, M, R)* | | | Additional criteria to determine peak/wave type (P or T) in R-R interval ($RR_t$)* | Discrimination of peak/wave type (P or T) present in R-R interval | | |
|---|---|---|---|---|---|---|---|---|---|---|---|
| | | 1st peak | 2nd peak | 3rd peak | 1st peak | 2nd peak | 3rd peak | | 1st peak | 2nd peak | 3rd peak |
| 17 | 1 | +ve/-ve | - | - | L/M | - | - | $RR_t$ with –ve $R_2$, or +ve $R_2$ with prominent S wave; $RR_t<(RR_{t-1}$ or $RR_{t+1})$; HR>100 bpm in $RR_t$ | T | - | - |
| 18 | 1 | +ve | - | - | L/M/R | - | - | $RR_t$ with +ve $R_1$ & –ve $R_2$; peak within 0.15 s of $R_2$ | T | - | - |
| 19 | 1 | -ve | - | - | R | - | - | $RR_t \approx RR_{t-1}$ | P | - | - |
| 20 | 1 | +ve | - | - | R | - | - | $RR_t$ with +ve $R_1$, $R_2$; $S_1$, $S_2$ > 0.24 mV; HR>100 bpm in $RR_t$ | T | - | - |
| 21 | 4 | -ve | +ve | -ve | L | L | M/R | $RR_t$ with +ve $R_1$, $R_2$; $S_1$, $S_2$ > 0.24 mV; HR>100 bpm in $RR_t$ | P | T | False +ve |
| | | | | +ve | | | R | | | | P |
| 22 | 1 | +ve | - | - | L/M | - | - | $RR_t$ with +ve $R_1$, $R_2$; QRS1(W) & QRS2(W) > 0.115 s | T | - | - |
| 23 | 1 | +ve | - | - | L | - | - | $RR_t$ with +ve $R_1$, $R_2$; $S_1$, $S_2$ < 0.24 mVor absent; QRS1(W) & QRS2(W) ≤ 0.115 s | P with undulations after it | | |
| 24 | 1 | +ve | - | - | M/R | - | - | $RR_t$ with +ve $R_1$ & -ve $R_2$; peak not within 0.15 s of $R_2$ | T | - | - |
| 0 | 0 | - | - | - | - | - | - | $RR_t$ with +ve $R_1$ & -ve $R_2$ | No peaks present | | |
| 100 | None of the above conditions fulfilled | | | | | | | | | | |

IJBST

ISSN: 0974 – 3987
IJBST (2009), 2(7): 96-125

Table 3. QRS features computed from MIT/BIH rec. no. 205
Duration: 1677.989-1684.3 sec

| QRS Features | 1 | 2 | 3 | 4 | 5 | 6 | 7 | 8 | 9 |
|---|---|---|---|---|---|---|---|---|---|
| QRSn (s) | 1678.264 | 1679.006 | 1679.703 | 1680.442 | 1681.172 | 1681.939 | 1682.311 | 1683.400 | 1684.136 |
| QRSna (mV) | 1.200 | 1.200 | 1.250 | 1.285 | 1.280 | 1.180 | 1.525 | 1.235 | 1.180 |
| Qs (s) | - | - | 1679.719 | 1680.464 | 1681.192 | - | - | 1683.414 | - |
| Qa (mV) | - | - | 1.155 | 1.220 | 1.200 | - | - | 1.140 | - |
| Qamp (mV) | - | - | 0.095 | 0.065 | 0.080 | - | - | 0.095 | - |
| Rs (s) | 1678.292 | 1679.031 | 1679.750 | 1680.492 | 1681.219 | 1681.967 | 1682.347 | 1683.442 | 1684.164 |
| Ra (mV) | 2.495 | 2.510 | 2.520 | 2.510 | 2.470 | 2.460 | 0.000 | 2.580 | 2.520 |
| Ramp (mV) | 1.295 | 1.310 | 1.270 | 1.225 | 1.190 | 1.280 | 1.525 | 1.345 | 1.340 |
| Rang (deg) | 2.446 | 2.412 | 2.343 | 2.315 | 2.505 | 2.460 | 6.173 | 2.228 | 2.359 |
| Ss (s) | 1678.311 | 1679.053 | 1679.767 | 1680.508 | 1681.239 | 1681.986 | - | 1683.461 | 1684.183 |
| Sa (mV) | 1.135 | 1.135 | 1.115 | 1.155 | 1.150 | 1.095 | - | 1.115 | 1.105 |
| Samp (mV) | 0.065 | 0.065 | 0.135 | 0.130 | 0.130 | 0.085 | - | 0.120 | 0.075 |
| Sang (deg) | 1.962 | 2.247 | 1.935 | 2.407 | 2.609 | 1.960 | - | 1.836 | 1.682 |
| R's (s) | 1678.328 | 1679.069 | - | 1680.528 | - | 1682.003 | - | 1683.475 | - |
| R'a (mV) | 1.405 | 1.370 | - | 1.395 | - | 1.365 | - | 1.355 | - |
| R'amp (mV) | 0.205 | 0.170 | - | 0.110 | - | 0.185 | - | 0.120 | - |
| QRSf (s) | 1678.353 | 1679.103 | 1679.781 | 1680.550 | 1681.258 | 1682.022 | 1682.447 | 1683.492 | 1684.197 |
| QRSfa (mV) | 1.285 | 1.280 | 1.335 | 1.290 | 1.375 | 1.250 | 1.500 | 1.260 | 1.375 |
| QRSfamp (mV) | 0.085 | 0.080 | 0.085 | 0.005 | 0.095 | 0.070 | 0.025 | 0.025 | 0.195 |
| QRS(W) (s) | 0.089 | 0.097 | 0.078 | 0.108 | 0.086 | 0.083 | 0.136 | 0.092 | 0.061 |
| VAT (s) | 0.028 | 0.025 | 0.047 | 0.050 | 0.047 | 0.028 | 0.036 | 0.042 | 0.028 |
| QRS config | RSR' | RSR' | QRS | QRSR' | QRS | RSR' | QS | QRSR' | RS |

* Refer list of symbols (Table 7) for description of variables listed in QRS features. '-' symbolizes absence of respective QRS feature in the corresponding QRS complex.

Table 4. R-R interval features computed from MIT/BIH rec. no. 205
Duration: 1677.989-1684.3 sec

| R-R Interval Features | R1-R2 | R2-R3 | R3-R4 | R4-R5 | R5-R6 | R6-R7 | R7-R8 | R8-R9 |
|---|---|---|---|---|---|---|---|---|
| R-R int | 0.739 | 0.719 | 0.742 | 0.727 | 0.748 | 0.380 | 1.095 | 0.722 |
| HR | 81.191 | 83.449 | 80.863 | 82.531 | 80.214 | 157.895 | 54.795 | 83.102 |
| FLAG | 1 | 1 | 1 | 1 | 1 | 0 | 1 | 1 |
| Pn (s) | 1678.853 | 1679.569 | 1680.303 | 1681.042 | 1681.783 | - | 1683.269 | 1683.975 |
| Pna (mV) | 1.272 | 1.265 | 1.286 | 1.297 | 1.264 | - | 1.236 | 1.272 |
| Ps (s) | 1678.900 | 1679.617 | 1680.358 | 1681.089 | 1681.836 | - | 1683.317 | 1684.033 |
| Pa (mV) | 1.323 | 1.316 | 1.353 | 1.343 | 1.320 | - | 1.281 | 1.332 |
| Pamp (mV) | 0.051 | 0.051 | 0.067 | 0.046 | 0.056 | - | 0.045 | 0.060 |
| Pf (s) | 1678.956 | 1679.675 | 1680.417 | 1681.147 | 1681.897 | - | 1683.367 | 1684.094 |
| Pfa (mV) | 1.243 | 1.227 | 1.271 | 1.261 | 1.231 | - | 1.223 | 1.249 |
| Pfamp (mV) | 0.029 | 0.038 | 0.015 | 0.036 | 0.033 | - | 0.013 | 0.023 |
| P-R int (s) | 0.153 | 0.134 | 0.139 | 0.130 | 0.156 | - | 0.131 | 0.161 |
| P-R seg (s) | 0.050 | 0.028 | 0.025 | 0.025 | 0.042 | - | 0.033 | 0.042 |
| P-P int (s) | 0.717 | 0.741 | 0.731 | 0.747 | - | - | 0.716 | - |
| AVCR | 1:1 | 1:1 | 1:1 | 1:1 | 1:1 | 0:1 | 1:1 | 1:1 |

* Refer list of symbols (Table 7) for description of variables listed in R-R interval features. '-' symbolizes absence of respective feature in the corresponding R-R interval.

IJBST

ISSN: 0974 – 3987
IJBST (2009), 2(7): 96-125

Table 5. QRS features computed from MIT/BIH rec. no. 202
Duration: 1107.333-1113.997 sec

| QRS Features | 1 | 2 | 3 | 4 | 5 | 6 |
|---|---|---|---|---|---|---|
| QRSn (s) | 1107.725 | 1108.889 | 1110.028 | 1111.139 | 1112.325 | 1113.525 |
| QRSna (mV) | 0.130 | 0.120 | 0.140 | 0.225 | 0.210 | 0.150 |
| Qs (s) | - | - | - | - | - | - |
| Qa (mV) | - | - | - | - | - | - |
| Qamp (mV) | - | - | - | - | - | - |
| Rs (s) | 1107.775 | 1108.942 | 1110.081 | 1111.186 | 1112.372 | 1113.578 |
| Ra (mV) | 2.165 | 2.070 | 2.100 | 2.200 | 2.140 | 2.245 |
| Ramp (mV) | 2.035 | 1.950 | 1.960 | 1.975 | 1.930 | 2.095 |
| Rang (deg) | 3.577 | 3.256 | 3.052 | 2.608 | 2.783 | 2.836 |
| Ss (s) | - | - | - | - | - | - |
| Sa (mV) | - | - | - | - | - | - |
| Samp (mV) | - | - | - | - | - | - |
| Sang (deg) | - | - | - | - | - | - |
| R's (s) | - | - | - | - | - | - |
| R'a (mV) | - | - | - | - | - | - |
| R'amp (mV) | - | - | - | - | - | - |
| QRSf (s) | 1107.833 | 1108.981 | 1110.114 | 1111.214 | 1112.403 | 1113.611 |
| QRSfa (mV) | 0.060 | 0.175 | 0.215 | 0.245 | 0.255 | 0.195 |
| QRSfamp (mV) | 0.070 | 0.055 | 0.075 | 0.020 | 0.045 | 0.045 |
| QRS(W) (s) | 0.108 | 0.092 | 0.086 | 0.075 | 0.078 | 0.086 |
| VAT (s) | 0.050 | 0.053 | 0.053 | 0.047 | 0.047 | 0.053 |
| QRS config | R | R | R | R | R | R |

* Refer list of symbols (Table 7) for description of variables listed in QRS features. '-' symbolizes absence of respective QRS feature in the corresponding QRS complex.

Table 6. R-R interval features computed from MIT/BIH rec. no. 202
Duration: 1107.333-1113.997 sec

| R-R Interval Features | R1-R2 | R2-R3 | R3-R4 | R4-R5 | R5-R6 |
|---|---|---|---|---|---|
| R-R int | 1.167 | 1.139 | 1.105 | 1.186 | 1.206 |
| HR | 51.414 | 52.678 | 54.299 | 50.590 | 49.751 |
| FLAG | 1 | 1 | 1 | 1 | 1 |
| Pn (s) | 1108.675 | 1109.836 | 1110.947 | 1112.111 | 1113.308 |
| Pna (mV) | 0.071 | 0.090 | 0.199 | 0.158 | 0.133 |
| Ps (s) | 1108.758 | 1109.908 | 1111.008 | 1112.183 | 1113.389 |
| Pa (mV) | 0.172 | 0.177 | 0.274 | 0.246 | 0.218 |
| Pamp (mV) | 0.101 | 0.087 | 0.075 | 0.088 | 0.085 |
| Pf (s) | 1108.825 | 1109.969 | 1111.078 | 1112.256 | 1113.456 |
| Pfa (mV) | 0.069 | 0.099 | 0.152 | 0.141 | 0.119 |
| Pfamp (mV) | 0.002 | 0.009 | 0.047 | 0.017 | 0.014 |
| P-R int (s) | 0.214 | 0.192 | 0.192 | 0.214 | 0.217 |
| P-R seg (s) | 0.064 | 0.059 | 0.061 | 0.069 | 0.069 |
| P-P int (s) | 1.150 | 1.100 | 1.175 | 1.206 | - |
| AVCR | 1:1 | 1:1 | 1:1 | 1:1 | 1:1 |

* Refer list of symbols (Table 7) for description of variables listed in R-R interval features. '-' symbolizes absence of respective feature in the corresponding R-R interval.

- The technique extracts the different characteristic points of the QRS complex and the P wave (QRS-onset, QRS-offset, P-onset, P-offset) within the tolerance limits recommended by the CSE Working Party. The composite method has the potential to detect 37 diagnostic features used by cardiologists to classify arrhythmias in lead II ECG signals, provided these signals have distinguishable QRS complexes and P waves contaminated by any type and amount of background noise, but with a baseline wander not exceeding 0.25 Hz.

## CONCLUSIONS

ECG signals exhibiting irregular waveforms are indicators of arrhythmic events that lead to life threatening rhythms, such as ventricular fibrillation, ventricular tachycardia and atrial fibrillation. For example, R-on-T PVC generally leads to serious ventricular tachycardia resulting in deadly ventricular flutter /fibrillation. Detecting a single arrhythmia is much simpler than detecting a combination of arrhythmias (in the same ECG signal), as a small number of features extracted is sufficient for interpretation. In real situations, as observed in the standard ECGs, abnormal rhythms and beats exist in combinations of two or more. This overlapping feature characteristic of arrhythmias makes it challenging to obtain adequate feature detection and classification.

In this paper, a composite methodology has been developed to perform cycle-by-cycle feature extraction from the given signal to enable computer-aided interpretation of different arrhythmias. This helps the cardiologist while diagnosing one arrhythmia at a time, or a combination of two or more arrhythmias coexisting in the signal. The developed technique has been applied to different signals of MIT/BIH Database. The QRS detection algorithm was validated using 32,800 beats of several records of the MIT/BIH database and a detection accuracy of 99.96% was achieved within the tolerance limits recommended by the CSE Working Party. The composite method for detection of both P and QRS wave features has been validated using all the 25 records for lead II of the CSE Dataset-3, before being applied to approximately 8000 beats of the MIT/BIH database, wherein nearly 2,96,000 P wave and QRS complex features were extracted and manually verified.

The technique eliminates most of the shortcomings of the existing methods for ECG feature extraction, and leads to the detection of a number of useful diagnostic features related to the depolarisation sequence of the heart. On the basis of this strong set of diagnostic features, not only the isolated abnormal beats or rhythms can be detected, but also combinations of normal /abnormal beats and rhythms, as they appear in an ECG signal, can be successfully interpreted. The methodology is dynamic and amenable to further refinements if needed by a cardiologist to extend its potential to detect as many arrhythmias as possible.

## ACKNOWLEDGEMENT

The authors wish to thank Dr. J.P.S. Sawhney, DM (Cardiology), Member American College of Cardiology and Senior Consultant Cardiologist at Sir Ganga Ram Hospital, New Delhi, India, for his valuable suggestions. The authors are also thankful to Dr. Praveen Gothi, MD (Medicine) Ex-Heart Specialist at Apollo Hospital, New Delhi, India, for his helpful guidance during the course of the work

## REFERENCES

[1] N. Goldschlager, and M.J. Goldman, (1989) Principles of clinical electrocardiography, 13th Edition, Appleton and Lange (Prentice Hall).

[2] G.S. Wagner, (1994) Marriott's practical electrocardiography, 9th Edition, B.I. Waverly Pvt. Ltd., New Delhi.

[3] D.J. Rowlands, (1991) Clinical electrocardiography, Gower Medical Publishing, London .

[4] A. Leatham, C. Bull, and M.V. Braimbridge, (1993) Lecture notes on cardiology, 3rd Edition, Blackwell Scientific Publications

[5] R.C. Schlant, and R.W. Alexander, (1995) Hurst's the heart, 8th Edition, McGraw-Hill

[6] W.J. Tompkins, (1999) Biomedical digital signal processing, Prentice-Hall of India..

[7] K. Lin, and W.H. Chang, (1989) QRS feature extraction using linear prediction, IEEE Trans. Biomed. Eng., 36: 1050-1055.

[8] M.S. Woolfson, (1991) Study of cardiac arrhythmia using the Kalman filter, Med. & Biol. Eng. & Comput., 29: 398-405.

[9] O. Weiben, V.X. Afonso, and W.J. Tompkins, (1999) Classification of premature ventricular complexes

using filter bank features, induction of decision trees and a fuzzy rule-based system, Med. & Biol. Eng. & Comput., 37: 560-565.

[10] O A. Bartolo, B.D. Clymer, R.C. Burgess, J.P. Turnbull, J.A. Golish, and M.C. Perry, (2001) An arrhythmia detector and heart rate estimator for overnight polysomnography studies, IEEE Trans. Biomed. Eng., 48:513-521.

[11] S. Osowski, and T.H. Linh,(2001) ECG beat recognition using fuzzy hybrid neural network, IEEE Trans. Biomed. Eng., 48: 1265-1271.

[12] J.S. Sahambi, S.N. Tandon, and R.K.P. Bhatt,(1997) Quantitative analysis of errors due to power-line interference and base-line drift in detection of onsets and offsets in ECG using wavelets, Med. & Biol. Eng. & Comput.,35: 747-751.

[13] J. Pan, and W.J. Tompkins,(1985) A real-time QRS detection algorithm, IEEE Trans. Biomed. Eng., 32:230-236.

[14] P.S. Hamilton, and W.J. Tompkins, (1986) Quantitative investigations of QRS detection rules using the MIT/BIH arrhythmia database, IEEE Trans. Biomed. Eng., 33:1157-1165.

[15] Q. Xue, H.H. Yu, and W.J. Tompkins, (1992) Neural-network-based adaptive matched filtering for QRS detection, IEEE Trans. Biomed. Eng., 39: 317-329.

[16] I.S.N. Murthy, and G.S.S.D. Prasad, (1992) Analysis of ECG from pole-zero models, IEEE Trans. Biomed. Eng., 39:741-751.

[17] R. Poli, S. Cagnoni, and G. Valli,(1995) Genetic design of optimum linear and nonlinear QRS detectors, IEEE Trans. Biomed. Eng., 42: 1137-1144.

[18] C. Li, C. Zheng, and C. Tai, (1995) Detection of ECG characteristic points using wavelet transform, IEEE Trans. Biomed. Eng., 42: 21-28.

[19] E.A. Botter, Jr. C.L. Nascimento, and T. Yoneyama,(2001) A neural network with asymmetric basis functions for feature extraction of ECG P waves, IEEE Trans. Biomed. Eng., 12: 1252-1255.

[20] L. Gang, Y. Wenyu, L. Ling, Y. Qilian, and Y. Xuemin,(2000) "An artificial-intelligence approach to ECG analysis", IEEE Eng. Med. & Biol., 95-100.

[21] I. Mohamed Owis, Ahmed H. Abou-Zied, Abou-Bakar M. Youssef, and Yasser M. Kadah, (2002) Study of features based on non-linear dynamical modeling in ECG arrhythmia detection and classification, IEEE Trans. BME, 49(7) : 733-736.

[22] Liang-Yu Shyu, Ying-Hsuan Wu, and Weichih Hu,(2004) Using wavelet transform and fuzzy neural network for VPC detection from the Holter ECG, IEEE Trans. BME, 51(7):1269-1273.

[23] Philip de Chazal, Maria O' Dwyer, and Richard B. Reilly,(2004) Automatic classification of heart beats using ECG morphology and heart beat interval features, IEEE Trans. BME, 51(7): 1196-1206.

[24] MIT/BIH Arrhythmia Database Directory,(1992) 3rd Edition, Harvard-MIT Division of Health Sciences and Technology.

[25] L. Khadra, A.S. Al-Fahoum, and H. Al-Nashash,(1997) Detection of life-threatening cardiac arrhythmias using the wavelet transformation, Med. & Biol. Eng. & Comput., 35: 626-632.

[26] P.K. Kulkarni,(1997) Ambulatory monitoring and analysis of ECG signals, Ph.D.thesis, Dept. of Elect. Engg., University of Roorkee, Roorkee, India.

[27] M.L. Ahlstrom, and W.J. Tompkins, (1985) Digital filters for real-time ECG signal processing using microprocessors, IEEE Trans. Biomed. Eng., 32: 708-713.

[28] J.E. Van Alste and T.S. Schilder, (1985) Removal of base-line wander and power line interference from the ECG by efficient FIR filter with a reduced number of taps, IEEE Trans. Biomed. Eng., 32: 1050-1060.

[29] L. Sornmo, (1993) Time-varying digital filtering of ECG baseline wander, Med. & Biol. Eng. & Comput., 31: 503-508.

[30] G.M. Friesen, T.C. Jannet, M.A. Jadallah, S.L. Yates, S.R. Quint, and H.T. Nagle,(1990) A comparison of the noise sensitivity of nine QRS detection algorithms, IEEE Trans. Biomed. Eng., 37: 85-98.

[31] N.V. Thakor, J.G. Webster, and W.J. Tompkins, (1984) Design, implementation and evaluation of a microcomputer-based portable arrhythmia monitor, Med. & Biol. Eng. & Comput., 22:151-159.

[32] L. Sornmo, and O. Pahlm, (1984) Software QRS detection in ambulatory monitoring – a review, Med. & Biol. Eng. & Comput., 22: 289-297.

[33] C.H. Chu and E.J. Delp,(1989) Impulsive noise suppression and background normalization of electrocardiogram signals using morphological operators, IEEE Trans. Biomed. Eng., 36: 262-273.

[34] J.L. Willems,(1988) CSE multilead atlas: measurement results -Data Set 3, CSE Project of the Commission of the European Communities.

[35] T. Fancott and D.H. Wong,(1980) A minicomputer system for direct high speed analysis of cardiac arrhythmia in 24h ambulatory ECG tape recordings, IEEE Trans. Biomed. Eng., 27: 685-693.

[36] S.C. Saxena, V. Kumar, and S.T. Hamde,(2002) QRS detection using new wavelets, J. Med. Eng. Tech.,26:7-15.

[37] I.K. Daskalov, I.A. Dotsinsky, and I.I. Christov, (1998) Developments in ECG acquisition, preprocessing,

parameter measurement, and recording, IEEE Eng. in Med. & Biol.,50-58.

[38] H.T. Le, W.C. Van Ardsel, A.M. Makowski, E.E. Pottala, and J.J. Bailey, (1985) Automated analysis of rodent three-channel electrocardiograms and vectorcardiograms, IEEE Trans. Bio. Med. Eng., 32: 43-49.

[39] J.L.Willems,(1985) Recommendations for measurement standards in quantitative electrocardiography, European Heart J., 6: 815-825.

[40] P. Trahanias, and E. Skordalakis, (1989) Bottom-up approach to the ECG pattern recognition problem, Med. & Biol. Eng. & Comput., 27:221-229.

[41] P. Trahanias, and E. Skordalakis,(1990) Syntactic pattern recognition of the ECG, IEEE Trans. Pattern Analysis & Machine Intelligence,12(7): 648-657.

[42] S.D. Stearns, and R.A. David,(1998) Signal processing algorithms, Prentice-Hall, Inc.,.

[43] P.W. Macfarlane, J. Peden, G. Lennex, M.P. Watts, and T.D.V. Lawrie,(1977) The Glasgow System, Proc. Trends in Computer-Processed Electro-Cardiograms, 143-150.

[44] B.R.S. Reddy, I.S.N. Murthy, and P.C. Chatterjee, (1985) Rhythm analysis using vectorcardiograms, IEEE Trans. Biomed. Eng., 32: 97-104.

[45] M. Stridh, and L. Sornmo,(2001) Spatiotemporal QRST cancellation techniques for analysis of atrial fibrillation, IEEE Trans. Biomed. Eng., 48:105-111.

[46] S. Mangiola, and M.C. Ritota,(1982) Cardiac arrhythmias: practical ECG interpretation, 2nd Edition, J.B. Lippincott Company.

[47] R. Maheshwari, G. Vijaya, V. Kumar, and H.K. Verma,(1998) Signal-analysis and heuro-logistic interpretation of multilead electrocardiograms, Inter. J. Systems Sci., 29: 323-334.

[48] Y. Wang, Y.-S. Zhu, N.V. Thakor, and Y.-H. Xu,(2001) A short-time multifractal approach for arrhythmia detection based on fuzzy neural network, IEEE Trans. Biomed. Eng., 48: 989-995.

[49] Illanes-Manriquez A. and Zhang Q.,(2008) An algorithm for robust detection of QRS onset and offset in ECG signals, Computers in Cardiology, 35:857-860.

Table 7. List of symbols

| *Symbol* | *Description* |
|---|---|
| AVCR | Atrio-ventricular conduction ratio |
| FLAG | Integer number (+ve) indicating the presence, polarity, position and number of P/T waves in an interval w.r.t. isoelectric line detected between successive QRS complexes and w.r.t. mid-point of RR interval |
| HR | Heart rate in beats per minute (bpm) |
| Pa | Amplitude (in mV) of P peak |
| Pamp | \|Pna - Pa\| |
| Pf | Location of P wave offset in seconds corresponding to a sample number |
| Pfa | Amplitude (in mV) of P wave offset |
| Pfamp | \|Pna - Pfa\| |
| Pn | Location of P wave onset in seconds corresponding to a sample number |
| Pna | Amplitude (in mV) of P wave onset |
| Ps | Location of P peak in seconds corresponding to a sample number |
| P-R int | Interval (in sec) between onset of P wave and onset of the following QRS complex |
| P-R seg | Interval (in sec) between offset of P wave and onset of the following QRS complex |
| P-P int | Interval (in sec) between onset of P wave and onset of the next P wave |
| Qa | Amplitude (in mV) of Q peak |
| Qamp | \|QRSna - Qa\| |
| Qs | Location of Q peak in seconds corresponding to a sample number |
| QRSf | Location of QRS complex offset in seconds corresponding to a sample number |
| QRSfa | Amplitude (in mV) of QRS complex offset |

| | |
|---|---|
| QRSfamp | \|QRSna - QRSfa\| |
| QRSn | Location of QRS complex onset in seconds corresponding to a sample number |
| QRSna | Amplitude (in mV) of QRS complex onset |
| QRS config | Configuration of QRS complex (i.e. QRSR′, QRS, QR, RSR′, RS, R, QS) |
| QRS(W) | Time duration or width (in sec) of QRS complex |
| Ra | Amplitude (in mV) of R peak |
| Ramp | \|QRSna - Ra\| |
| Rang | Angle of R peak (in degrees) |
| Rs | Location of R peak in seconds corresponding to a sample number |
| R'a | Amplitude (in mV) of R' peak |
| R'amp | \|QRSna – R'a\| |
| R's | Location of R' peak in seconds corresponding to a sample number |
| R-R int | Interval (in sec) between two consecutive R peaks |
| Sa | Amplitude (in mV) of S peak |
| Samp | \|QRSna - Sa\| |
| Sang | Angle of S peak (in degrees) |
| Ss | Location of S peak in seconds corresponding to a sample number |
| VAT | Ventricular activation time |